





Article

SNP-Based Genetic Analysis of Dimensional Stability and Wood Density in *Eucalyptus pellita* F.Muell. and Hybrids

Oluwatosin Esther Falade ¹, Benoit Belleville ¹, Antanas Spokevicius ¹, Barbara Ozarska ^{1,*}, Gerd Bossinger ¹, Listya Mustika Dewi ¹, Umar Ibrahim ¹ and Bala Thumma ²

¹ School of Agriculture, Food and Ecosystem Sciences, Faculty of Science, University of Melbourne, Melbourne, VIC 3010, Australia; oluwatosin.falade@student.unimelb.edu.au (O.E.F.); benoit.belleville@unimelb.edu.au (B.B.); avjs@unimelb.edu.au (A.S.); gerd@unimelb.edu.au (G.B.); ldewi@student.unimelb.edu.au (L.M.D.); umaribrahim.suliankatchisha@student.unimelb.edu.au (U.I.)

² Diversity Arrays Technology, University of Canberra, Monana Street, Bruce, ACT 2617, Australia; balat@diversityarrays.com

* Correspondence: bo@unimelb.edu.au

Abstract

Dimensional stability is a key trait for structural wood applications such as flooring, yet its genetic basis in *Eucalyptus pellita* F.Muell. and its hybrids remain poorly understood. Addressing this gap is essential for improving processing efficiency and product quality through targeted breeding. This study assessed variation in shrinkage and density, their relationships with growth and chemical traits, and associated genetic markers. Wood samples from *E. pellita*, *E. pellita* × *E. urophylla* S.T.Blake, and *E. pellita* × *E. brassiana* S.T.Blake were collected from two plantation sites in northern Australia. Radial and tangential shrinkage and density were measured alongside growth and chemical traits. SNP genotyping was conducted to identify markers linked to these physical properties. Significant differences were observed among hybrid types. *E. pellita* × *E. urophylla* recorded the lowest tangential unit shrinkage (0.06%), while *E. pellita* × *E. brassiana* had the highest basic density (651 kg/m³). Shrinkage and density showed moderate to strong correlations with growth and chemical traits. Several SNPs were associated with these properties; all were located in the intergenic region near *Eucgr.A00211*. Among these, only one SNP exceeded the $-\log_{10}(p)$ significance threshold. These results provide early genetic insights and potential candidate markers for improving wood quality in *Eucalyptus* breeding programs. This exploratory study, constrained by a small sample size ($n = 58$), identifies putative SNPs for future validation in broader, multi-environment trials.

Keywords: *Eucalyptus pellita*; hybrids; shrinkage; density; growth traits; chemical traits; genetic markers



Academic Editors: Pablo Lopez-Albarran and José Guadalupe Rutiaga-Quinones

Received: 24 May 2025

Revised: 5 August 2025

Accepted: 6 August 2025

Published: 9 August 2025

Citation: Falade, O.E.; Belleville, B.; Spokevicius, A.; Ozarska, B.; Bossinger, G.; Dewi, L.M.; Ibrahim, U.; Thumma, B. SNP-Based Genetic Analysis of Dimensional Stability and Wood Density in *Eucalyptus pellita* F.Muell. and Hybrids. *Forests* **2025**, *16*, 1301. <https://doi.org/10.3390/f16081301>

Copyright: © 2025 by the authors. Licensee MDPI, Basel, Switzerland. This article is an open access article distributed under the terms and conditions of the Creative Commons Attribution (CC BY) license (<https://creativecommons.org/licenses/by/4.0/>).

1. Introduction

Plantations of fast-growing trees are increasingly established worldwide to address wood shortages caused by the decline of natural forests. In Australia, planted forests have become a vital source of wood and fiber, now constituting a larger share of the harvestable supply as industrial wood from native forests continues to decline [1–4]. While hardwood plantations were initially established to supply wood chips for the pulp and paper industry, the sector has expanded to produce higher-value products such as sawn and engineered wood [3]. Among these, *Eucalyptus* species are increasingly valued for solid wood applications where dimensional stability is essential. This property, which

reflects how wood responds to changes in moisture, directly affects product performance, durability, and market value [5,6]. As such, improving dimensional stability has become a key target in hardwood plantation breeding programs.

Among *Eucalyptus* species, *Eucalyptus pellita* F.Muell. (red mahogany), a Myrtaceae species endemic to Queensland, Australia, is well-suited for humid, tropical, and subtropical environments. Its performance in field trials has confirmed its suitability for plantation forestry in these regions [7,8]. Breeding programs aim to boost productivity by selecting superior genotypes for hybridization and clonal propagation. This improves wood properties for construction, pulp, and bioenergy applications [9–11]. In Indonesia, hybrids such as *E. grandis* W.Hill ex Maiden \times *E. pellita* (G \times P) and *E. grandis* \times *E. urophylla* S.T.Blake (G \times U) have been evaluated for key properties, including basic density, shrinkage, compressive strength, and modulus of elasticity and rupture. The G \times P hybrid exhibited improved compressive strength and consistent wood quality without compromising growth, highlighting the potential of hybridization to enhance timber properties [12]. Similarly, trials involving *E. urophylla* \times *E. pellita* hybrids reported combined benefits in growth adaptability and performance, with minimal reductions in wood quality [13]. By selecting superior genotypes and optimizing breeding strategies, the program aims to improve growth rates and wood quality, fostering a more sustainable and profitable timber industry. This approach positions *Eucalyptus pellita* as a valuable resource for diverse industrial applications.

Numerous studies have examined genetic and phenotypic relationships between growth and wood traits using non-destructive tree evaluation. Most research has focused on growth traits and wood properties influencing pulp yield, such as basic density, cellulose, hemicellulose, lignin, and extractives [10]. However, wood quality is not defined by a single index. Dimensional stability, which describes how wood shrinks and swells with moisture changes, is crucial for various product applications, especially in applications exposed to fluctuating between dry and humid seasons [14–16]. Along with density and other properties, it plays a key role in determining wood quality. Genetically, density and pulp yield are typically controlled by fewer, more additive loci and often show strong correlations with growth traits [17,18]. In contrast, dimensional stability is influenced by a complex combination of anatomical features, including microfibril angle and fiber structure, and chemical components such as hemicellulose–lignin interactions, which tend to be under polygenic control and more affected by environmental variation [19,20]. These differences make dimensional stability a more challenging trait to assess and improve through conventional selection methods, requiring targeted genetic studies to enable its integration into tree breeding programs.

While these properties are well studied, their genetic basis, particularly in *Eucalyptus pellita*, remains unexplored. In *E. globulus*, studies using genetic correlations, genetic algorithms and near-infrared models have revealed significant heritability for pulpwood and shrinkage-related traits, highlighting the feasibility of indirect selection for stability [21–23]. In *Pinus koraiensis* Zuccarini and Siebold, clonal trials demonstrated moderate to high heritability for wood quality traits, supporting multi-trait selection strategies [24]. In *E. grandis*, genomic modification [25] has been studied to enhance dimensional stability. Although effective, these treatments increase embodied carbon or involve non-renewable chemicals, limiting recyclability. Tree breeding offers a sustainable alternative, improving dimensional stability without environmental drawbacks [26], which can be fast-tracked using emerging genomic technologies. Selection has improved predictive accuracy for rarely measured traits such as pulp yield and cellulose [27], while *E. urograndis* hybrids have shown strong genetic control of wood properties, such as density, cellulose and lignin, using SNP-based models [28]. Similarly, in *Larix kaempferi* Lamb., provenance trials identified genotypes combining superior growth and wood stability traits [29]. Despite these advances, such genetic

insights remain limited for *E. pellita* and its hybrids. The absence of studies identifying SNPs for dimensional stability in this species represents a key research gap. Understanding the genetic basis of this trait could support targeted breeding for high-performance timber suitable for variable climatic conditions.

Several methods, such as chemical [30–32], thermal [33,34], and metal ion modification [25], have been investigated to enhance dimensional stability in wood products. While often effective, these treatments may increase production costs, involve non-renewable or toxic substances, and reduce product recyclability, thereby limiting their environmental and economic sustainability. In contrast, tree breeding offers a more cost-effective and eco-friendly solution by genetically improving dimensional stability at the source. This approach aligns with long-term plantation management goals and can be accelerated through the use of genomic technologies such as GWAS and SNP-based selection [26]. For example, Tan and Ingvarsson [17] found that SNPs selected from a genome-wide association study (GWAS) in *Eucalyptus* result in improving the prediction abilities of estimated breeding values for traits like density and pulp yield [17]. However, the lack of information on SNPs related to dimensional stability in *E. pellita* and its hybrids highlights the need for targeted genetic association studies on physical wood properties. Such studies could enhance selection efficiency and support both industry demand and environmental sustainability.

Further research is needed to understand the genetic basis of dimensional stability and its relationship with other wood traits in *E. pellita* and its hybrids. Despite its importance in product performance, this trait remains poorly studied at the molecular level in this species. This study addresses that gap by integrating phenotypic assessment of shrinkage and density with genomic data to identify markers associated with dimensional stability. The specific objectives were to (i) evaluate density and shrinkage variation in parent trees and hybrids, (ii) explore the relationships between physical properties, growth traits, and chemical components, and (iii) identify molecular markers linked to density and dimensional stability. By combining genomic and phenotypic data, this work provides a novel framework for improving selection efficiency in breeding programs targeting dimensional stability and supports the development of more resilient, high-value plantation resources. Given the limited sample size ($n = 58$), this study is considered exploratory, with the identified SNPs representing promising candidates for future validation in expanded genetic trials.

2. Materials and Methods

2.1. Sampling Area

This study was carried out on two *E. pellita* trial sites in the Tiwi Islands, Northern Territory, Australia: Kilu Impini 64 (KI64) and Yapilika 28 (YP28) (Table 1). Both sites were established in 2012 using a randomized complete block design, with four complete replicates and 25 trees per replicate, resulting in a total of 1000 trees planted per site. The trials were spaced at 3×3 m to balance stand density. Standard silvicultural practices, including weed control, pruning, and thinning, were applied uniformly across both sites. The two sites were selected to represent contrasting environmental conditions in terms of soil type, elevation, and exposure, enabling assessment of genotype \times environment interactions.

Table 1. Location and description of research trial sites.

	Kilu Impini 64	Yapilika 28
Coordinates	11°25'6.00" S 130°30'0.00" E	11°33'45.00" S 130°34'39.00" E
Rainfall	1200–1400 mm	1200–1400 mm
Number of seedlots	10	10
Year planted	2012	2012
Number of trees planted	1000	1000
Number of living trees (Year 2022)	763	666
Soil	Red sandy soils and gray to yellow sandy soil > 2 m	Moonkinu Member sandstone > 3 m
Tree/plot	25	25
Replications	4	4
Spacing	3 × 3 m	3 × 3 m

2.2. Genetic Material and Trial Establishment

Growth traits (height and diameter at breast height) were measured on 1429 trees across two sites, with 763 trees at Kilu Impini 64 and 666 trees at Yapilika 28 plantation sites. DNA samples and wood chips were collected for genotyping, identifying five genetic groups: *E. pellita*, first-generation hybrids (*E. pellita* × *E. brassiana* (F1), *E. pellita* × *E. urophylla* (F1)), and backcross hybrids (*E. pellita* × *E. brassiana* (BC), *E. pellita* × *E. urophylla* (BC)), as summarized in Table 2. F1 hybrids result from two parent species, while BC hybrids are F1 crosses with one parent. These hybrids were distributed across 10 seedlots. The hybrid groups were selected to evaluate the potential for genetic gain in tropical plantations. Prior breeding work has shown that incorporating other *Eucalyptus* into *E. pellita* breeding populations can enhance adaptability, disease resistance, and wood quality in tropical environments. Including F1 and BC hybrids enabled the evaluation of heterosis and trait inheritance relevant to productivity and product development.

Table 2. Number of trees genotyped and selected for shrinkage and density assessment per genotype group and site.

Hybrid/Genotype Group	Total Genotyped	Kilu Impini 64	Yapilika 28	Selected Trees: Kilu Impini 64	Selected Trees: Yapilika 28
<i>E. pellita</i>	858	456	402	6	6
<i>E. pellita</i> × <i>E. brassiana</i> (BC)	97	59	38	6	6
<i>E. pellita</i> × <i>E. brassiana</i> (F1)	25	17	8	6	5
<i>E. pellita</i> × <i>E. urophylla</i> (BC)	313	160	153	6	6
<i>E. pellita</i> × <i>E. urophylla</i> (F1)	136	71	65	6	5
Total	1429	763	666	30	28

F1: first-generation hybrid; BC: backcross hybrid.

Cambial tissue was collected from the tree trunk using a chisel, as this layer contains actively dividing cells rich in nuclear DNA and is suitable for high-throughput field-based genotyping. DNA was extracted using a modified cetyltrimethylammonium bromide (CTAB) protocol, following Tibbits et al. [35], which facilitates efficient tissue collection and high-yield DNA isolation from mature trees. Genotyping was performed by Gondwana Genomics using a Targeted Genotyping-by-Sequencing (TGS) method with a custom *E. pellita* SNP panel. This method involved capturing targeted regions with oligonucleotide probes, amplification of the captured regions using universal primers, and sequencing on an Illumina platform (Illumina Inc., San Diego, USA) with an average read depth of approximately 30× per locus. A raw dataset of 5500 SNP markers per individual was generated

and provided for downstream genetic structure and association analyses. These SNPs were aligned to the *Eucalyptus grandis* reference genome (v2.0, Phytozome) for downstream genetic structure and association analyses.

2.3. Estimation of Physical Properties

Trees with diameter at breast height (Dbh) greater than 15 cm were selected from the genotyped population. Within each genotype group, individuals were grouped into three wood density classes (high, medium, low) using a 3-bar histogram based on non-destructive wood density measurements obtained with a Resistograph, IML Resi PD400 (IML System GmbH, Wiesloch, Germany). From these classes, trees were randomly selected at both sites. Trees exhibiting defects (e.g., multiple stems, termite damage, or decayed cores) were excluded. A total of 30 trees were selected from Kilu Impini 64 and 28 trees from Yapilika 28, ensuring representation across all genotype groups and density classes (Table 2). While six trees were targeted per group per site, only five trees were selected for each of the F1 hybrid groups on Yapilika 28 due to limited population sizes. This limited replication was the result of resource constraints and the need to balance sampling intensity with destructive harvesting and detailed processing. Nevertheless, the sampling design was structured to maximize representation across genotype and density classes while ensuring adequate phenotypic coverage for trait analysis. At 10 years of age, the selected trees were felled, and basal discs (~50 mm thick) were collected at 100 mm above ground level. The discs were placed in sealed plastic bags and stored in insulated cooler boxes for transport.

Dimensional stability (shrinkage) was assessed according to the methods described by Kingston and Risdon [36], which outline best practices for evaluating shrinkage from the green state to specified moisture levels under controlled environmental conditions. Each green disc was processed into 2 tangential and radial shrinkage samples per tree, with nominal dimensions of 25 mm (thickness) \times 100 \pm 2 mm (length) \times 25 mm (width), as shown in Figure 1. Samples were labeled by anatomical orientation and sealed in plastic bags to minimize moisture loss before initial measurements. Dimensions were measured using digital calipers (precision \pm 0.01 mm) and weight was recorded using a digital balance (precision \pm 0.01 g).

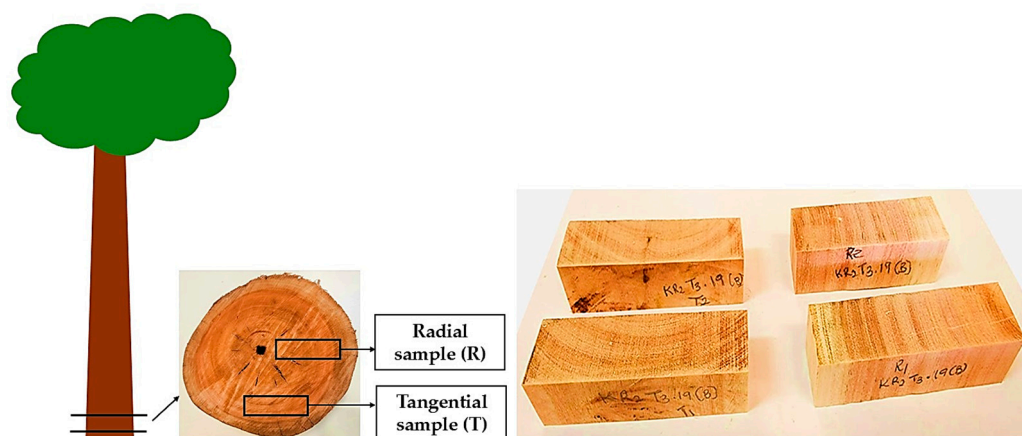


Figure 1. Collection of tangential and radial samples from a disc.

After machining, green samples were conditioned to 17% moisture content (MC) at 23 °C and 85% relative humidity (RH) in a conditioning chamber until equilibrium moisture content (EMC) was reached. Weight and dimensions were recorded. Samples were then conditioned to 12% MC at 23 °C and 65% RH, with measurements repeated at EMC. The samples were reconditioned in an autoclave to relieve stress, after which samples were returned to 12% MC and then conditioned to 5% MC at 30 °C and 55% RH. Measurements

were taken after reaching EMC at each stage. Finally, the samples were oven-dried at 103 °C for 24 h. Shrinkage (SH) was calculated at 17% MC, 12% MC before reconditioning (BR), 12% MC after reconditioning (AR), and 5% MC. Shrinkage (SH) at each moisture level was calculated using the following:

$$SH(\%) = \frac{I_d - F_d}{I_d} \quad (1)$$

where I_d is the initial dimension at the green stage (mm), and F_d is the final dimension at any moisture content (mm).

Unit shrinkage was calculated between 12% MC and 5% MC as shown below:

$$US(\%) = \frac{\Delta D}{\Delta MC} \quad (2)$$

where ΔD is the change in dimension (%) and ΔMC is the change in moisture content.

The density of wood samples was determined according to ASTM D2395 [37] based on precise dimensional measurements (length, width, thickness) and mass. The weight and volume of the samples were measured in both green and oven-dry conditions. Green density (ρ_{\max}), oven-dry density (ρ_o), and basic density (ρ_b) were calculated using the following:

$$\rho_{\max} = \frac{m_{\max}}{V_{\max}} \quad (3)$$

where m_{\max} is the green mass of the test piece (kg) and V_{\max} is the green volume of the test piece (m^3).

$$\rho_o = \frac{m_o}{V_o} \quad (4)$$

where m_o is the dry mass of the test piece (kg), and V_o is the oven-dried volume of the test piece (m^3).

$$\rho_b = \frac{m_o}{V_{\max}} \quad (5)$$

2.4. Correlation Between Physical Property, Growth, and Chemical Property Traits

Growth traits, total height, and diameter at breast height (DBH) were measured at age 10 prior to harvesting. DBH was recorded at 1.3 m using a diameter tape, and total height was measured using a Nikon Forestry Pro II laser rangefinder, following standard field protocols across both sites. Chemical traits were assessed using near-infrared spectroscopy (NIRS). Wood chips were collected from the outer stem behind the cambium at breast height (± 130 cm), oven-dried, and milled to obtain 16-mesh woodmeal. Approximately 1 g of each sample was scanned using a Bruker MPA FT-NIR instrument across the 4000–10,000 wavenumber range. Calibrations for Klason lignin, total lignin, cellulose, extractives, and kraft pulp yield (KPY) were developed using partial least squares regression (PLSR) with the Bruker QUANT package within the OPUS 5.5 software (Bruker Optik, Ettlingen, Germany) following protocols by Poke and Raymond [38] and Downes et al. [39]. Models with $R^2 > 0.80$ and residual predictive deviation (RPD) > 2.0 were retained. Box plots were used to evaluate data distribution and detect outliers, and traits showed approximately normal distributions with linear relationships. Pearson correlation analysis was performed using individual tree-level data ($n = 58$) to assess relationships among growth, chemical, and physical wood traits. Understanding the correlation between these traits provides key insights into how growth and chemical properties influence physical traits (Table 3), which are essential determinants of wood suitability for various applications.

Table 3. Physical properties, growth traits, and chemical component traits abbreviations.

Abbreviations	Full Meaning
Physical properties traits	
Sh17_T	Shrinkage from green to 17% MC in tangential direction
Sh17_R	Shrinkage from green to 17% MC in radial direction
Sh12BR_T	Shrinkage from green to 12% MC before reconditioning in tangential direction
Sh12BR_R	Shrinkage from green to 12% MC before reconditioning in radial direction
Sh12AR_T	Shrinkage from green to 12% MC after reconditioning in tangential direction
Sh12AR_R	Shrinkage from green to 12% MC after reconditioning in radial direction
Sh5_T	Shrinkage from green to 5% MC in tangential direction
Sh5_R	Shrinkage from green to 5% MC in radial direction
US_T	Unit shrinkage in tangential direction
US_R	Unit shrinkage in radial direction
GD_T	Green density at tangential direction
GD_R	Green density in radial direction
OD_T	Oven-dry density in tangential direction
OD_R	Oven-dry density in radial direction
BD_T	Basic density in tangential direction
BD_R	Basic density in radial direction
Growth traits	
Ht	Height
Dbh_t	Diameter at breast height measured with tape
Dbh_r	Diameter at breast height measured with Resistograph
Chemical component traits	
KPY	Kraft pulp yield
TL	Total lignin
KL	Klason lignin
Ext	Extractives
Cel	Cellulose

2.5. Assessment of Phenotypic Variation and Genetic Association

Phenotypic shrinkage data were first analyzed using mixed linear models (MLMs) in R (version 4.3.3) to evaluate the effects of hybrid group and plantation sites. Hybrid group and plantation sites were treated as fixed effects, and individual tree was modeled as a random effect, allowing for the assessment of phenotypic variation across genetic backgrounds and environments. An SNP-based genetic association analysis was then conducted using shrinkage and density observations from 58 trees, combined with approximately 5500 SNPs generated using the *E. pellita* marker panel developed by Gondwana Genomics [40]. SNPs with multiple mutations or a minor allele frequency (MAF) below 0.10 were filtered using TASSEL (version 5.2.93), resulting in a final dataset of approximately 3000 high-quality SNPs. The MAF threshold was selected to minimize the inclusion of rare alleles and improve statistical power, given the limited sample size. The association analysis was implemented using the GAPIT (version 3) R package with the BLINK method [41,42], which iteratively includes associated markers as covariates and re-tests for significance to reduce false positives caused by cryptic relatedness. To control population structure and relatedness, a kinship matrix was generated using the VanRaden method, and the first three principal components (PCs) derived from the SNP marker matrix were included as covariates. These PCs were selected based on scree plot inspection and collectively explained 38.6% of the total genetic variance. Population origin group was also included using binary indicator variables, with the last group omitted to avoid linear dependence. Missing genotype data were imputed using the major allele method available in GAPIT. Multiple testing was controlled using the Benjamini–Hochberg false discovery rate (FDR)

correction [43], with significance set at an adjusted $p < 0.05$. SNP positions were aligned to the *Eucalyptus grandis* reference genome version 2.0 (Phytozome), which serves as a pseudo-reference due to its high synteny with *E. pellita*.

3. Results and Discussion

3.1. Phenotypic Variation in Shrinkage Property Traits

The hybrids evaluated in this study comprised first-generation (F1) crosses between *Eucalyptus pellita* and either *E. urophylla* or *E. brassiana*, as well as backcrosses (BCs) produced by crossing the F1 progeny back to *E. pellita*.

Results showed significant variation in shrinkage, with values higher in the tangential direction than in the radial direction for all hybrids, as expected (Table 4). This reflects the anisotropic nature of wood; the tangential shrinkage tends to be greater due to the arrangement of fibers, orientation of ray cells, and the influence of growth rings. These anatomical features limit movement in the radial direction more than the tangential, leading to the observed directional differences [14]. At KI64, *E. pellita* × *E. urophylla* (F1) had the lowest unit shrinkage (0.16% T, 0.08% R) with confidence interval of 0.11%–0.22% at T and 0.01%–0.15% at R (Table A1). The highest shrinkage in the tangential direction was in *E. pellita* × *E. brassiana* (F1) (0.21%), and in the radial direction, *E. pellita* had the highest (0.18%). At YP28, *E. pellita* × *E. brassiana* (F1) had the lowest unit shrinkage (0.11% T, 0.09% R) with confidence interval of 0.07%–0.15% at T and 0.01%–0.16% at R (Table A1). The highest unit shrinkage in the tangential direction was in *E. pellita* × *E. brassiana* (BC) (0.22%), and in the radial direction, *E. pellita* × *E. urophylla* (F1) had the highest (0.18%).

Table 4. Means, LSD, and p -values for shrinkage values among the hybrids at Kilu Impini 64 (KI64) and Yapilika 28 (YP28), and the combined plantation sites.

Plantation Sites/Hybrids	Green to 17% (%)		Green to 12% BR (%)		Green to 12% AR (%)		Green to 5% (%)		Unit Shrinkage (%)	
	T	R	T	R	T	R	T	R	T	R
KI64										
<i>E. pellita</i>	2.31 ^a (0.56)	1.20 ^a (0.24)	4.00 ^a (0.57)	2.16 ^a (0.41)	3.00 ^a (0.54)	1.45 ^a (0.40)	6.14 ^a (0.44)	4.67 ^a (0.63)	0.20 ^a (0.02)	0.18 ^a (0.02)
<i>E. pellita</i> × <i>E. brassiana</i> (BC)	3.86 ^a (0.62)	1.60 ^a (0.29)	5.27 ^a (0.62)	2.71 ^a (0.49)	4.34 ^a (0.61)	2.34 ^a (0.47)	6.67 ^a (0.47)	4.58 ^a (0.74)	0.19 ^a (0.02)	0.15 ^a (0.03)
<i>E. pellita</i> × <i>E. brassiana</i> (F1)	4.09 ^a (0.71)	1.75 ^a (0.26)	5.70 ^a (0.75)	3.30 ^a (0.44)	4.26 ^a (0.69)	2.60 ^a (0.43)	7.49 ^a (0.59)	4.79 ^a (0.68)	0.21 ^a (0.02)	0.13 ^a (0.03)
<i>E. pellita</i> × <i>E. urophylla</i> (BC)	2.33 ^a (0.54)	1.49 ^a (0.22)	3.95 ^a (0.55)	2.95 ^a (0.38)	2.96 ^a (0.52)	2.02 ^a (0.36)	5.76 ^a (0.43)	4.09 ^a (0.58)	0.19 ^a (0.02)	0.13 ^a (0.02)
<i>E. pellita</i> × <i>E. urophylla</i> (F1)	3.48 ^a (0.65)	1.42 ^a (0.30)	5.05 ^a (0.68)	2.36 ^a (0.51)	4.05 ^a (0.63)	1.99 ^a (0.49)	6.65 ^a (0.53)	3.27 ^a (0.77)	0.16 ^a (0.02)	0.08 ^a (0.03)
LSD ($p = 0.05$)	2.14	0.85	2.18	1.45	2.08	1.40	1.69	2.22	0.07	0.10
LSD ($p = 0.05$)—Tukey	3.15	1.22	3.16	2.08	3.06	2.01	2.42	3.18	0.10	0.14
p -value YP28	0.15	0.62	0.23	0.41	0.27	0.41	0.20	0.60	0.68	0.24
YP28										
<i>E. pellita</i>	2.01 ^a (0.42)	1.42 ^a (0.17)	3.54 ^a (0.41)	2.56 ^a (0.26)	2.86 ^a (0.37)	2.13 ^a (0.26)	6.04 ^a (0.34)	4.69 ^a (0.47)	0.21 ^a (0.01)	0.15 ^a (0.03)
<i>E. pellita</i> × <i>E. brassiana</i> (BC)	3.29 ^a (0.55)	1.36 ^a (0.21)	4.88 ^a (0.51)	2.51 ^a (0.33)	3.11 ^a (0.44)	1.87 ^a (0.31)	6.93 ^a (0.43)	3.54 ^a (0.56)	0.22 ^a (0.01)	0.11 ^a (0.03)
<i>E. pellita</i> × <i>E. brassiana</i> (F1)	6.83 ^b (0.78)	3.01 ^b (0.21)	8.06 ^b (0.75)	4.21 ^a (0.33)	7.09 ^b (0.67)	3.84 ^a (0.31)	8.70 ^b (0.64)	4.56 ^a (0.56)	0.11 ^b (0.02)	0.09 ^a (0.03)
<i>E. pellita</i> × <i>E. urophylla</i> (BC)	2.30 ^a (0.46)	1.29 ^a (0.18)	3.92 ^a (0.45)	2.68 ^a (0.27)	2.99 ^a (0.41)	2.28 ^a (0.28)	6.28 ^a (0.38)	4.59 ^a (0.51)	0.22 ^a (0.01)	0.16 ^a (0.03)
<i>E. pellita</i> × <i>E. urophylla</i> (F1)	3.63 ^a (0.55)	1.57 ^a (0.39)	4.88 ^a (0.53)	2.44 ^a (0.60)	3.94 ^a (0.47)	2.14 ^a (0.62)	6.47 ^a (0.45)	4.85 ^a (1.21)	0.16 ^a (0.01)	0.18 ^a (0.06)

Table 4. Cont.

Plantation Sites/Hybrids	Green to 17% (%)		Green to 12% BR (%)		Green to 12% AR (%)		Green to 5% (%)		Unit Shrinkage (%)	
	T	R	T	R	T	R	T	R	T	R
LSD ($p = 0.05$)	2.00	0.94	1.93	1.44	1.72	1.46	1.63	2.65	0.05	0.15
LSD ($p = 0.05$)—Tukey	2.88	1.35	2.78	2.08	2.49	2.11	2.35	3.84	0.07	0.22
p -value	0.00	0.00	0.00	0.01	0.00	0.00	0.02	0.55	0.00	0.45
Plantation combined										
<i>E. pellita</i>	2.16 ^a (0.28)	1.33 ^a (0.29)	3.74 ^a (0.30)	2.38 ^a (0.31)	2.93 ^a (0.30)	1.86 ^a (0.32)	6.03 ^a (0.33)	4.60 ^a (0.34)	0.20 ^a (0.01)	0.16 ^a (0.02)
<i>E. pellita</i> × <i>E. brassiana</i> (BC)	3.64 ^b (0.29)	1.48 ^a (0.31)	5.32 ^b (0.31)	2.60 ^a (0.33)	3.91 ^b (0.32)	2.16 ^a (0.33)	7.03 ^a (0.34)	4.05 ^a (0.36)	0.20 ^a (0.02)	0.13 ^a (0.02)
<i>E. pellita</i> × <i>E. brassiana</i> (F1)	5.15 ^c (0.38)	2.33 ^a (0.29)	6.55 ^c (0.41)	3.72 ^b (0.31)	5.34 ^c (0.41)	3.15 ^a (0.32)	8.00 ^b (0.45)	4.64 ^a (0.34)	0.19 ^a (0.02)	0.11 ^a (0.02)
<i>E. pellita</i> × <i>E. urophylla</i> (BC)	2.34 ^a (0.29)	1.42 ^a (0.29)	3.96 ^a (0.31)	2.85 ^a (0.31)	3.02 ^a (0.31)	2.17 ^a (0.31)	6.03 ^a (0.34)	4.40 ^a (0.34)	0.21 ^a (0.02)	0.14 ^a (0.02)
<i>E. pellita</i> × <i>E. urophylla</i> (F1)	3.52 ^b (0.29)	1.15 ^a (0.42)	4.84 ^b (0.33)	2.14 ^a (0.46)	4.07 ^b (0.34)	1.81 ^a (0.46)	6.49 ^a (0.36)	3.41 ^a (0.50)	0.16 ^a (0.02)	0.11 ^a (0.02)
LSD ($p = 0.05$)	0.97	1.03	1.04	1.11	1.04	1.11	1.13	1.21	0.05	0.05
LSD ($p = 0.05$)—Tukey	1.36	1.45	1.46	1.56	1.45	1.55	1.59	1.69	0.07	0.07
Site	0.15		0.31		0.14		0.36		0.96	
Hybrid	0.00		0.00		0.00		0.08		0.28	
Position	0.00		0.00		0.00		0.00		0.00	
Site × Hybrid	0.03		0.18		0.04		0.70		0.25	
Site × Position	0.79		0.92		0.75		0.61		0.71	
Hybrid × Position	0.00		0.00		0.04		0.00		0.33	
Site × Hybrid × Position	0.50		0.49		0.45		0.38		0.17	

F1: first-generation hybrid; BC: backcross; BR: Before reconditioning; AR: After reconditioning; T: Tangential; R: Radial. Level of significance ($p < 0.05$), Confidence level used = 0.95, hybrids that are not significantly different from each other have the same letter, while hybrids that are significantly different from each other have different letters (based on the Tukey LSD).

Shrinkage is critical in determining wood quality, especially for structural applications exposed to varying moisture conditions [14]. Tangential shrinkage is more pronounced than radial shrinkage, leading to differential stresses and increasing the likelihood of deformation [44]. Evaluating both directions reveals wood stability under varying moisture conditions, crucial for product performance. Shrinkage from green to 17% MC occurs as free and bound water is removed. Bound water is lost below the fiber saturation point (FSP), marking the start of shrinkage and indicating initial drying stability [45].

For shrinkage from green to 17% MC, values ranged from 2.16% to 5.15% in the T direction, with *E. pellita* showing the lowest shrinkage, and from 1.15% to 2.33% in the R direction. Significant differences were observed among hybrids for shrinkage from green to 17% MC, 12% BR, and 12% AR in both T and R directions at the YP28 site. At KI64, no significant differences were found.

The Tukey test at YP28 revealed significant differences. *E. pellita* × *E. brassiana* (F1) had higher shrinkage than other hybrids in both tangential and radial directions for shrinkage from green to 17% MC. It also showed significantly higher shrinkage at 12% BR, 12% AR, and 5% MC. Other hybrids, like *E. pellita*, *E. pellita* × *E. brassiana* (BC), *E. pellita* × *E. urophylla* (BC), and *E. pellita* × *E. urophylla* (F1), had no significant differences (Table 4).

Assessing shrinkage at 12% BR and AR is crucial for understanding the wood's dimensional stability during drying. Shrinkage BR provides insights into contraction under standard drying conditions, while shrinkage AR reflects the wood's ability to recover from internal stress, improving stability and reducing defects [35,36]. Shrinkage from green to 12% AR is lower compared to 12% BR, indicating stress relief and improved dimensional stability. Tangential shrinkage exceeding 5%, an industry threshold for acceptable dimen-

sional stability, is generally considered to increase the risk of warping in structural wood [6]. In this study, tangential shrinkage values observed for some hybrids, particularly at 12% moisture content, were below this threshold, indicating improved dimensional stability. Shrinkage at 5% MC helps evaluate wood performance in low-humidity environments. Unit shrinkage ranged from 0.16% to 0.21% in the T direction and 0.11% to 0.16% in the R direction. *E. pellita* × *E. urophylla* (F1) had the lowest shrinkage. These values were lower than those reported for older trees [12,46] and those reported by WoodSolutions [47], suggesting the effect of age on shrinkage.

Across sites, F1 hybrids, especially those with *E. urophylla* genetics, showed lower unit shrinkage than BCs and parent trees, suggesting a potential benefit of incorporating *E. urophylla* genetics for improving dimensional stability. Within KI64, no significant differences in shrinkage were observed among genotype groups, indicating that the relatively uniform environmental conditions at this site may have masked genetic effects. This site is characterized by deep red and yellow sandy soils (>2 m), which likely provide consistent drainage and moisture availability, potentially reducing environmental stress and limiting the expression of genotype-specific traits. In contrast, greater variability in shrinkage was observed at YP28, where some differences among genotype groups were more apparent. The site's underlying Moonkinu Member sandstone (>3 m) may lead to more heterogeneous moisture and nutrient availability, creating conditions where genetic differences are more readily expressed. Although both sites receive similar annual rainfall (1200–1400 mm), the contrasting soil profiles likely influence growth dynamics and wood formation. These findings suggest that the expression of shrinkage traits is context-dependent and may be more detectable under variable or suboptimal site conditions. When data from both sites were analyzed collectively (Table 4), hybrid effects remained significant, indicating consistent genetic influence on shrinkage across the environment. However, the overall site effect was not significant (e.g., $p = 0.959$ for unit shrinkage), likely due to opposing or neutralizing hybrid responses across sites, which masked any main environmental effect.

A study conducted in South Asia (tropical climate) reported tangential and radial shrinkage of 5.15% and 3.35% in 12-year-old *E. brassiana* at 12% MC, increasing to 7.57% and 5.80% under oven-dry conditions [48,49]. These values are comparable to those observed for *E. pellita* × *E. brassiana* in this study, suggesting similar anatomical traits such as cell wall thickness and microfibril angle (MFA), which influence transverse shrinkage. In contrast, *E. urophylla* grown in tropical/subtropical climates exhibited higher shrinkage (10.34% tangential, 6.50% radial) [50] than *E. pellita* × *E. urophylla* hybrids. This may be due to species-specific differences in MFA, growth rate, or cell wall development, with hybrids potentially inheriting more stable traits from *E. pellita*. Interestingly, shrinkage values reported for 11-year-old *E. urophylla* and *E. urophylla* × *E. grandis* from temperate regions [51] were closely aligned with those observed for *E. pellita* × *E. urophylla* in this study. This similarity may reflect the effects of slower growth and higher wood density commonly associated with cooler climates. In addition, the superior dimensional stability observed in *E. pellita* × *E. urophylla* may be attributed to hybrid vigor, which can result in improved wood properties compared to the parental species. Hybrid vigor (heterosis) often enhances traits such as growth, wood quality, and adaptability, making hybrids valuable candidates for both breeding and commercial applications. The study also highlighted that unit shrinkage in eucalypts is governed by cell wall proportion, microfibril angle (MFA), and double fiber wall thickness. Meanwhile, total shrinkage is influenced by cell wall proportion, ray parenchyma content, and MFA, whereas residual shrinkage is particularly affected by the proportion of ray parenchyma [51]. These results underscore that shrinkage variation in *Eucalyptus* hybrids is shaped by genetic factors, growing environment, wood maturity, and underlying anatomical structures.

Differences in shrinkage from green to 12% MC before (BR) and after reconditioning (AR) have important implications for wood processing. Shrinkage during initial drying (BR) is influenced by anatomical features such as cell wall thickness, microfibril angle (MFA), and moisture retention capacity [52,53]. Juvenile wood, usually characterized by higher MFA and thinner fiber walls, tends to shrink more. After reconditioning, shrinkage at 12% MC (AR) is typically reduced due to partial stress relief and moisture redistribution. Ray parenchyma may also contribute by aiding internal stress recovery. Reconditioning improves dimensional stability, reduces defects, and enhances product quality [54–57]. In summary, understanding shrinkage behavior before and after reconditioning offers insights for improving wood quality, stability, and suitability across a wide range of applications.

3.2. Green Density, Oven-Dry Density, and Basic Density

At the KI64 site, green density (GD) ranged from 1044 kg/m³ (*E. pellita*) to 1156 kg/m³ (*E. pellita* × *E. brassiana* (BC)), and oven-dry density (OD) ranged from 587 kg/m³ (*E. pellita* × *E. urophylla* (BC)) to 781 kg/m³ (*E. pellita* × *E. brassiana* (F1)). Basic density (BD) ranged from 531 kg/m³ (*E. pellita*) to 643 kg/m³ (*E. pellita* × *E. brassiana* (BC)). At YP28, GD ranged from 1041 kg/m³ (*E. pellita*) to 1155 kg/m³ (*E. pellita* × *E. brassiana* (BC)), OD ranged from 582 kg/m³ (*E. pellita*) to 765 kg/m³ (*E. pellita* × *E. brassiana* (BC)), and BD ranged from 526 kg/m³ (*E. pellita*) to 638 kg/m³ (*E. pellita* × *E. brassiana* (BC)). Although *E. pellita* × *E. brassiana* (BC) consistently exhibited the highest density values across both sites, no significant differences were detected among hybrids within each site ($p > 0.05$), as shown in Table 5.

Table 5. Means, LSD, and p -values for density values among the hybrids at Kilu Impini 64 (KI64) and Yapilika 28 (YP28), and the combined plantation sites.

Plantation Sites/Hybrids	Green Density (kg/m ³)		Oven-Dry Density (kg/m ³)		Basic Density (kg/m ³)	
	T	R	T	R	T	R
KI64						
<i>E. pellita</i>	1085.00 ^a (24.40)	1044.00 ^a (16.60)	701.00 ^a (33.80)	589.00 ^a (28.80)	593.00 ^a (26.80)	531.00 ^a (24.60)
<i>E. pellita</i> × <i>E. brassiana</i> (BC)	1156.00 ^a (25.90)	1085.00 ^a (19.50)	766.00 ^a (34.80)	647.00 ^a (32.80)	643.00 ^a (27.90)	573.00 ^a (27.80)
<i>E. pellita</i> × <i>E. brassiana</i> (F1)	1136.00 ^a (33.40)	1090.00 ^a (17.90)	781.00 ^a (47.20)	626.00 ^a (33.30)	627.00 ^a (37.20)	553.00 ^a (28.60)
<i>E. pellita</i> × <i>E. urophylla</i> (BC)	1087.00 ^a (23.80)	1058.00 ^a (15.10)	695.00 ^a (33.80)	587.00 ^a (26.30)	588.00 ^a (26.50)	534.00 ^a (22.40)
<i>E. pellita</i> × <i>E. urophylla</i> (F1)	1093.00 ^a (29.40)	1069.00 ^a (20.30)	693.00 ^a (40.20)	605.00 ^a (36.60)	571.00 ^a (32.10)	545.00 ^a (31.30)
LSD ($p = 0.05$)	93.64	58.12	129.40	110.15	102.65	93.85
LSD ($p = 0.05$)—Tukey	134.15	83.30	184.90	160.85	146.75	136.75
p -value	0.23	0.35	0.36	0.60	0.41	0.81
YP28						
<i>E. pellita</i>	1103.00 ^a (22.20)	1041.00 ^a (19.80)	682.00 ^a (28.80)	582.00 ^a (24.30)	579.00 ^a (22.00)	526.00 ^a (20.00)
<i>E. pellita</i> × <i>E. brassiana</i> (BC)	1155.00 ^a (23.80)	1114.00 ^a (23.60)	765.00 ^a (33.40)	673.00 ^a (29.40)	638.00 ^a (26.40)	599.00 ^a (24.40)
<i>E. pellita</i> × <i>E. brassiana</i> (F1)	1108.00 ^a (35.90)	1065.00 ^a (23.70)	742.00 ^a (51.20)	631.00 ^a (29.50)	596.00 ^a (40.10)	551.00 ^a (24.50)
<i>E. pellita</i> × <i>E. urophylla</i> (BC)	1120.00 ^a (23.60)	1056.00 ^a (21.30)	750.00 ^a (31.60)	619.00 ^a (26.00)	620.00 ^a (24.20)	551.00 ^a (21.3)
<i>E. pellita</i> × <i>E. urophylla</i> (F1)	1117.00 ^a (25.40)	1104.00 ^a (46.90)	716.00 ^a (35.50)	663.00 ^a (57.20)	606.00 ^a (27.80)	591.00 ^a (47.00)

Table 5. Cont.

Plantation Sites/Hybrids	Green Density (kg/m ³)		Oven-Dry Density (kg/m ³)		Basic Density (kg/m ³)	
	T	R	T	R	T	R
LSD ($p = 0.05$)	93.50	111.21	131.62	135.95	102.75	111.85
LSD ($p = 0.05$)—Tukey	135.40	160.55	189.90	196.10	148.05	181.30
p -value	0.50	0.21	0.37	0.22	0.52	0.24
Plantation sites combined						
<i>E. pellita</i>	1090.00 ^a (13.90)	1038.00 ^a (14.40)	685.00 ^a (19.30)	583.00 ^a (19.70)	583.00 ^a (15.20)	527.00 ^a (15.50)
<i>E. pellita</i> × <i>E. brassiana</i> (BC)	1162.00 ^b (14.60)	1103.00 ^a (15.10)	788.00 ^b (20.20)	666.00 ^a (20.60)	651.00 ^a (15.90)	591.00 ^a (16.30)
<i>E. pellita</i> × <i>E. brassiana</i> (F1)	1135.00 ^b (18.50)	1084.00 ^a (14.60)	764.00 ^a (23.60)	628.00 ^a (20.20)	615.00 ^a (19.10)	552.00 ^a (15.90)
<i>E. pellita</i> × <i>E. urophylla</i> (BC)	1109.00 ^a (14.40)	1057.00 ^a (14.40)	726.00 ^a (21.90)	604.00 ^a (21.90)	607.00 ^a (17.10)	543.00 ^a (17.10)
<i>E. pellita</i> × <i>E. urophylla</i> (F1)	1124.00 ^a (15.50)	1082.00 ^a (20.50)	736.00 ^a (21.40)	627.00 ^a (25.80)	612.00 ^a (16.80)	564.00 ^a (20.90)
LSD ($p = 0.05$)	47.55	50.35	64.38	67.52	51.16	53.86
LSD ($p = 0.05$)—Tukey	66.67	70.57	90.45	94.80	71.83	75.55
Site	0.36		0.63		0.69	
Hybrid	0.01		0.03		0.06	
Position	0.00		0.00		0.00	
Site × Hybrid	0.86		0.83		0.91	
Site × Position	0.95		0.34		0.35	
Hybrid × Position	0.95		0.69		0.96	
Site × Hybrid × Position	0.262		0.416		0.540	

F1: first-generation hybrid; BC: backcross hybrid; T: Tangential; R: Radial. Level of significance ($p < 0.05$), Confidence level used = 0.95, hybrids that are not significantly different from each other have the same letter, while hybrids that are significantly different from each other have different letters (based on the Tukey LSD).

In summary, GD ranged from 1038 kg/m³ to 1162 kg/m³, OD ranged from 583 kg/m³ to 688 kg/m³, and BD ranged from 527 kg/m³ to 651 kg/m³. The 95% confidence intervals for these values are presented in Table A2. These values align with those reported for *E. pellita* in Borneo, Malaysia [58,59]. The hybrid *E. pellita* × *E. brassiana* (BC) exhibited the highest values for green, oven-dry, and basic densities. F1 hybrids had smaller sample sizes but tended to show intermediate to high-density values. The *E. brassiana* BC and F1 hybrids consistently had higher densities, suggesting a positive contribution of *E. brassiana* genetics to wood density.

The hybrid-specific basic density ranges observed in this study, from 527 kg/m³ (*E. pellita*) to 651 kg/m³ (*E. pellita* × *E. brassiana* hybrids), have practical implications for both dimensional stability and wood processing. Higher density, as exhibited by *E. brassiana* BC and F1 hybrids, is typically associated with greater strength and stiffness, which improves performance in structural applications and can enhance resistance to shrinkage-related deformation. However, higher-density wood may require slower and more controlled drying to minimize internal stress, checking, or collapse. In contrast, lower-density hybrids may dry and machine more easily but could be more prone to warping or reduced mechanical performance [53,60]. These findings underscore the importance of tailoring processing protocols, such as drying schedules, sawing strategies, and end-use decisions, based on the density profiles of individual hybrid groups.

When data from both sites were analyzed together (Table 5), hybrid effects on wood density were statistically significant ($p < 0.05$), indicating a consistent genetic influence. In contrast, site effects were not significant (e.g., $p = 0.06$ for basic density), suggesting

similar average densities across locations. Although some hybrid combinations showed higher density values, the differences were modest, with overlapping confidence intervals (e.g., 522.00–606.00 for *E. pellita* × *E. urophylla* (F1)), implying limited biological importance. These findings indicate that genetic variation had a greater influence on wood density than site conditions, consistent with the results reported by Li et al. [61].

These results have practical implications for tree selection and plantation management. *E. pellita* × *E. brassiana* hybrids, which showed higher density, may be more suitable for producing high-strength timber for structural uses such as construction and flooring. Conversely, hybrids with lower density, like *E. pellita* and *E. pellita* × *E. urophylla*, are more suitable for applications where lightweight wood is preferred. The lack of significant differences at individual sites highlights the role of environmental factors in influencing wood properties. However, even slight density variations among hybrids can affect drying and machining in certain processing contexts. While these differences may not require major changes to industrial practices, recognizing them can still support process optimization. Environmental influence also suggests density is mainly controlled by genetics, making it a reliable trait for selection and improvement [39,62–64].

3.3. Phenotypic Correlation

Pearson correlation analysis was conducted to examine relationships among physical, growth, and chemical traits. This provides insights into factors influencing wood suitability for industrial applications. The correlation matrix (Table 6) and heatmap (Figure 2) highlight strong positive correlations between shrinkage and density. Additionally, it shows negative correlations between shrinkage and both growth traits and some chemical components (TL, KL, and Ext. Sh12BR_T and Sh12AR_T were positively correlated with OD_T ($p = 0.02$), while Sh5_T showed significant correlations with GD_R ($p = 0.03$), OD_T ($p = 0.00$), OD_R ($p = 0.00$), and BD_R ($p = 0.02$). Similarly, Sh5_R correlated with OD_T ($p = 0.04$), OD_R ($p = 0.01$), and BD_R ($p = 0.04$).

Unit shrinkage in the tangential (US_T) and radial (US_R) directions also demonstrated associations with multiple density traits. These findings underscore the impact of density on dimensional changes during drying, which has important implications for processing and plantation management [60]. High-density wood is more prone to shrinkage, necessitating advanced drying techniques to minimize defects. The observed correlations reinforce the well-established relationship between wood density and shrinkage. This is critical for dimensional stability in industrial applications [54,65–67].

The significant correlations between shrinkage and growth traits suggest that faster-growing eucalyptus trees tend to exhibit higher shrinkage. US_T was strongly correlated with Ht ($p = 0.00$), Dbh_t ($p = 0.00$), and Dbh_r ($p = 0.00$), while US_R correlated with Ht ($p = 0.04$). Additionally, BD_R showed a positive correlation with Ht ($p = 0.02$). This indicates that taller trees tend to have denser wood in the radial direction, enhancing mechanical properties for structural applications [68–70]. These findings emphasize the need for optimized drying schedules to improve stability in fast-growing plantation trees. Shrinkage traits (Sh12BR_R, ShAR12_R, Sh5_R) also exhibited strong positive correlations with KPY ($p = 0.01$ – 0.04), suggesting that higher shrinkage may be associated with increased pulp yield. Denser wood often contains more cellulose per unit volume, which contributes to higher pulp recovery [21,71,72]. Positive correlations between shrinkage traits (Sh12BR_R, ShAR12_R, BD_T) and cellulose indicate that trees with higher cellulose content may also exhibit greater shrinkage. This influences their suitability for fiber production. These insights guide breeding strategies to balance growth, wood stability, and chemical composition for both solid wood and pulp applications.

Table 6. Correlation between physical property traits, growth traits, and chemical components at the combined plantation sites.

	GD_T	GD_R	OD_T	OD_R	BD_T	BD_R	Ht	Dbh_t	Dbh_r	KPY	TL	KL	Ext	Cel
Sh17_T	0.03	0.17	0.18	0.14	0.01	0.07	−0.13	−0.43 *	−0.43 *	0.04	−0.10	−0.08	−0.09	0.16
Sh17_R	−0.13	0.06	−0.01	0.02	−0.16	−0.05	−0.45 *	−0.71 *	−0.71 *	0.20	−0.49 *	−0.31 *	−0.37 *	0.20
Sh12BR_T	0.11	0.20	0.32 *	0.25	0.14	0.17	−0.07	−0.40 *	−0.40 *	0.06	−0.08	−0.07	−0.10	0.18
Sh12BR_R	−0.16	0.02	0.05	0.08	−0.08	0.01	−0.34 *	−0.61 *	−0.61 *	0.38 *	−0.54 *	−0.43 *	−0.45 *	0.39 *
Sh12AR_T	0.12	0.19	0.33 *	0.26	0.17	0.18	−0.07	−0.45 *	−0.45 *	0.03	−0.04	−0.05	−0.23	0.14
Sh12AR_R	0.06	0.19	0.23	0.28	0.11	0.20	−0.27	−0.56 *	−0.56 *	0.36 *	−0.45 *	−0.40 *	−0.44 *	0.30 *
Sh5_T	0.18	0.33 *	0.45 *	0.45 *	0.27	0.36 *	0.08	−0.26	−0.26	0.10	−0.05	−0.02	−0.08	0.19
Sh5_R	0.08	0.13	0.31 *	0.36 *	0.28	0.30 *	0.14	−0.11	−0.11	0.30 *	−0.25	−0.26	−0.39 *	0.23
US_T	0.29 *	0.30 *	0.35 *	0.44 *	0.42 *	0.47 *	0.41 *	0.48 *	0.48 *	0.01	0.10	0.10	0.12	−0.08
US_R	0.13	0.07	0.25	0.28 *	0.31 *	0.28	0.30 *	0.27	0.27	0.03	0.13	0.08	−0.05	−0.04
GD_T		0.67 *	0.81 *	0.64 *	0.86 *	0.62 *	0.01	−0.09	−0.09	−0.19	0.17	0.23	0.04	−0.16
GD_R			0.63 *	0.79 *	0.62 *	0.81 *	0.18	0.01	0.01	−0.19	0.01	0.11	0.03	−0.11
OD_T				0.84 *	0.96 *	0.80 *	0.20	−0.07	−0.07	−0.14	0.12	0.20	0.00	−0.09
OD_R					0.80 *	0.98 *	0.27	0.05	0.05	−0.12	0.06	0.13	−0.01	−0.05
BD_T						0.78 *	0.17	−0.02	−0.02	−0.21	0.19	0.28 *	0.05	−0.17
BD_R							0.33 *	0.14	0.14	−0.17	0.15	0.21	0.04	−0.09

* Significant at $p \leq 0.05$; Sh17_T: Shrinkage from green to 17% MC in tangential direction; Sh17_R: Shrinkage from green to 17% MC in radial direction; Sh12BR_T: Shrinkage from green to 12% MC before reconditioning in tangential direction; Sh12BR_R: Shrinkage from green to 12% MC before reconditioning in radial direction; Sh12AR_T: Shrinkage from green to 12% MC after reconditioning in tangential direction; Sh12AR_R: Shrinkage from green to 12% MC after reconditioning in radial direction; Sh5_T: Shrinkage from green to 5% MC in tangential direction; Sh5_R: Shrinkage from green to 5% MC in radial direction; US_T: Unit shrinkage in tangential direction; US_R: Unit shrinkage in radial direction; GD_T: Green density at tangential direction; GD_R: Green density in radial direction; OD_T: Oven-dry density in tangential direction; OD_R: Oven-dry density in radial direction; BD_T: Basic density in tangential direction; BD_R: Basic density in radial direction; Ht: Height; Dbh_t: Diameter at breast height measured with tape; Dbh_r: Diameter at breast height measured with Resi; KPY: Kraft pulp yield; TL: Total lignin; KL: Klason lignin; Ext: Extractives; Cel: Cellulose.

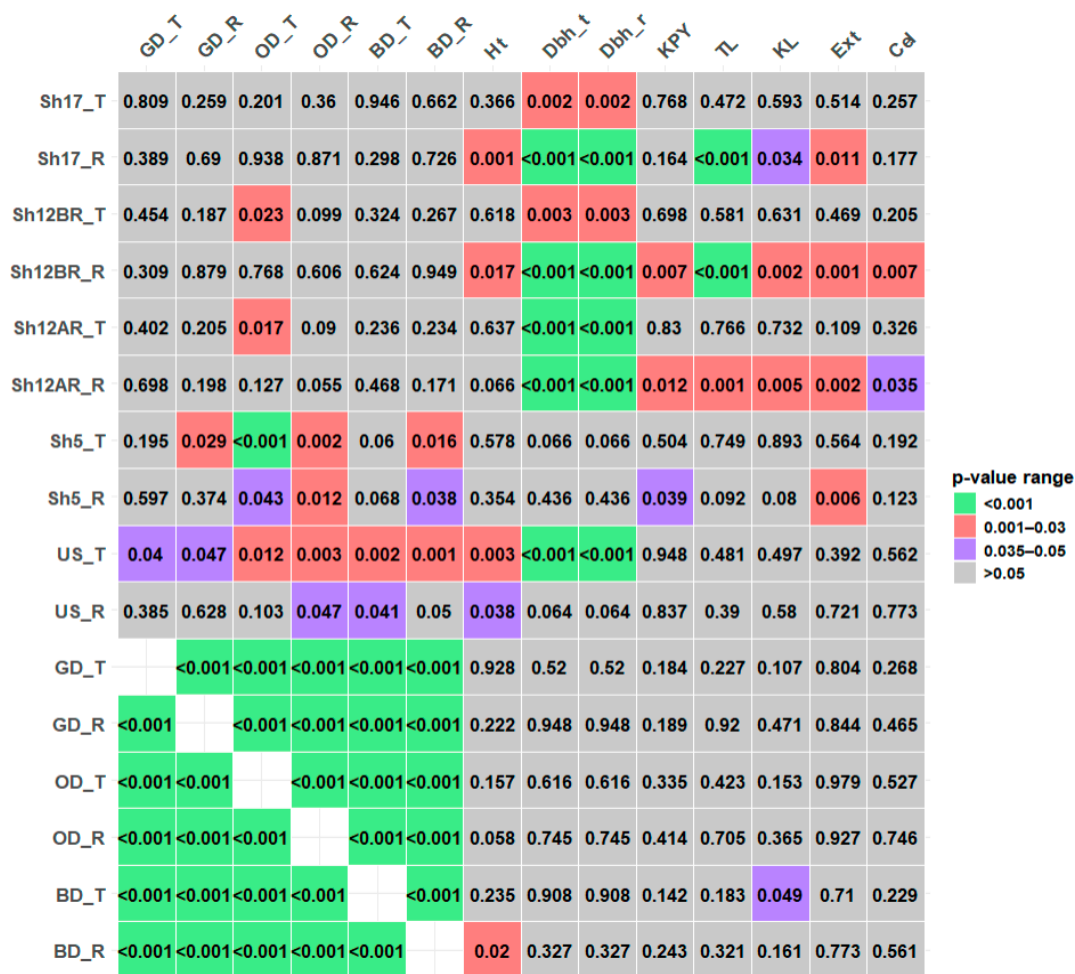


Figure 2. Correlation matrix for combined plantation sites between shrinkage properties, density, growth traits, and chemical components.

Conversely, significant negative correlations were found between shrinkage and both growth and chemical traits. Sh17_R and Sh12BR_R negatively correlated with Ht ($p = 0.00$, 0.02), while multiple shrinkage traits (Sh17_T, Sh17_R, Sh12BR_T, Sh12BR_R, Sh12AR_T, Sh12AR_R) exhibited significant negative correlations with Dbh_t and Dbh_r ($p = 0.00$ for all). Additionally, Sh17_R, Sh12BR_R, and Sh12AR_R were negatively correlated with TL, KL, and Ext ($p = 0.00$ – 0.03), with Sh5_R also negatively correlated with Ext ($p = 0.01$). These trends suggest that fast-growing trees tend to experience lower shrinkage. This could reduce drying defects but may also indicate lower wood density, impacting mechanical performance [73,74]. The negative correlation between shrinkage and chemical components suggests that wood with higher lignin and extractives may be more dimensionally stable [75,76]. These findings provide early insights into the interplay among growth, shrinkage, and chemical composition. Breeding programs should aim to optimize timber quality by mitigating shrinkage while maintaining sufficient density for industrial applications [14,65].

3.4. Manhattan and Q-Q Plots for Wood Shrinkage and Density Traits

Moderate genetic diversity was observed in the limited population used in this study. Individual heterozygosity peaked at 0.30–0.35, while most markers showed heterozygosity between 0.30 and 0.40. Minor allele frequencies peaked at 0.20–0.25, indicating moderate variation. Manhattan and quantile-quantile (Q-Q) plots illustrate SNP associations with wood properties. The Manhattan plots (Figures 3 and 4) show associations with shrinkage

at different moisture content (MC) levels (green to 17%, 12% before reconditioning (BR), 12% after reconditioning (AR), 5%, and unit shrinkage). Figure 5 showed associations with density traits (GD, OD, BD in tangential (T) and radial (R) directions). Peaks in these plots indicate varying levels of association.

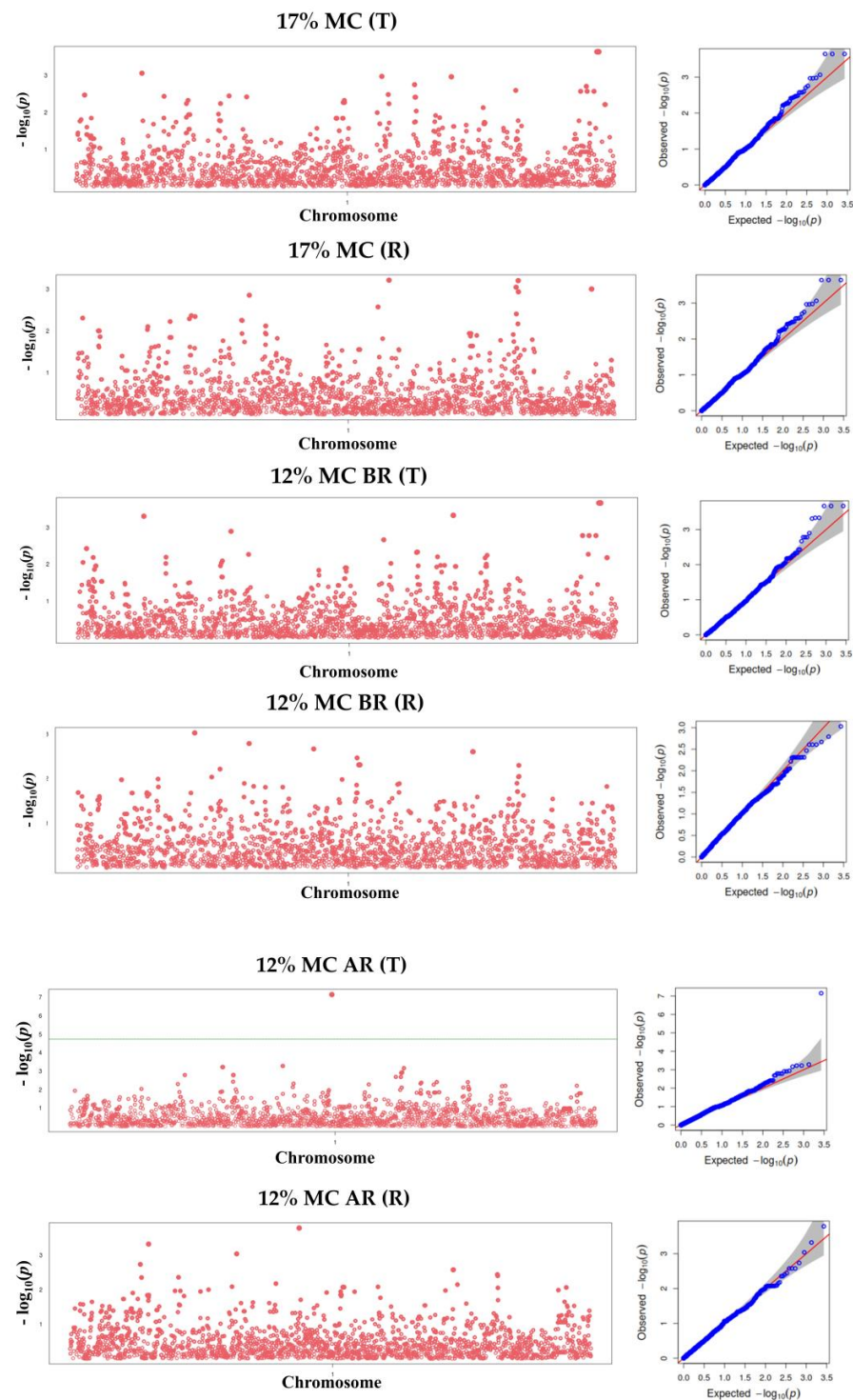


Figure 3. Manhattan and quantile-quantile (Q-Q) plots showing SNP associations with tangential (T) and radial (R) shrinkage at green to 17% moisture content (MC), 12% MC before reconditioning (BR), and 12% MC after reconditioning (AR). In the Manhattan plots (left), each red dot represents an individual SNP, with its genomic position on the x-axis and the $-\log_{10}(p)$ value on the y-axis. In the Q-Q plots (right), blue dots represent observed p -values compared to the expected distribution under the null hypothesis. The red line indicates the expected distribution.

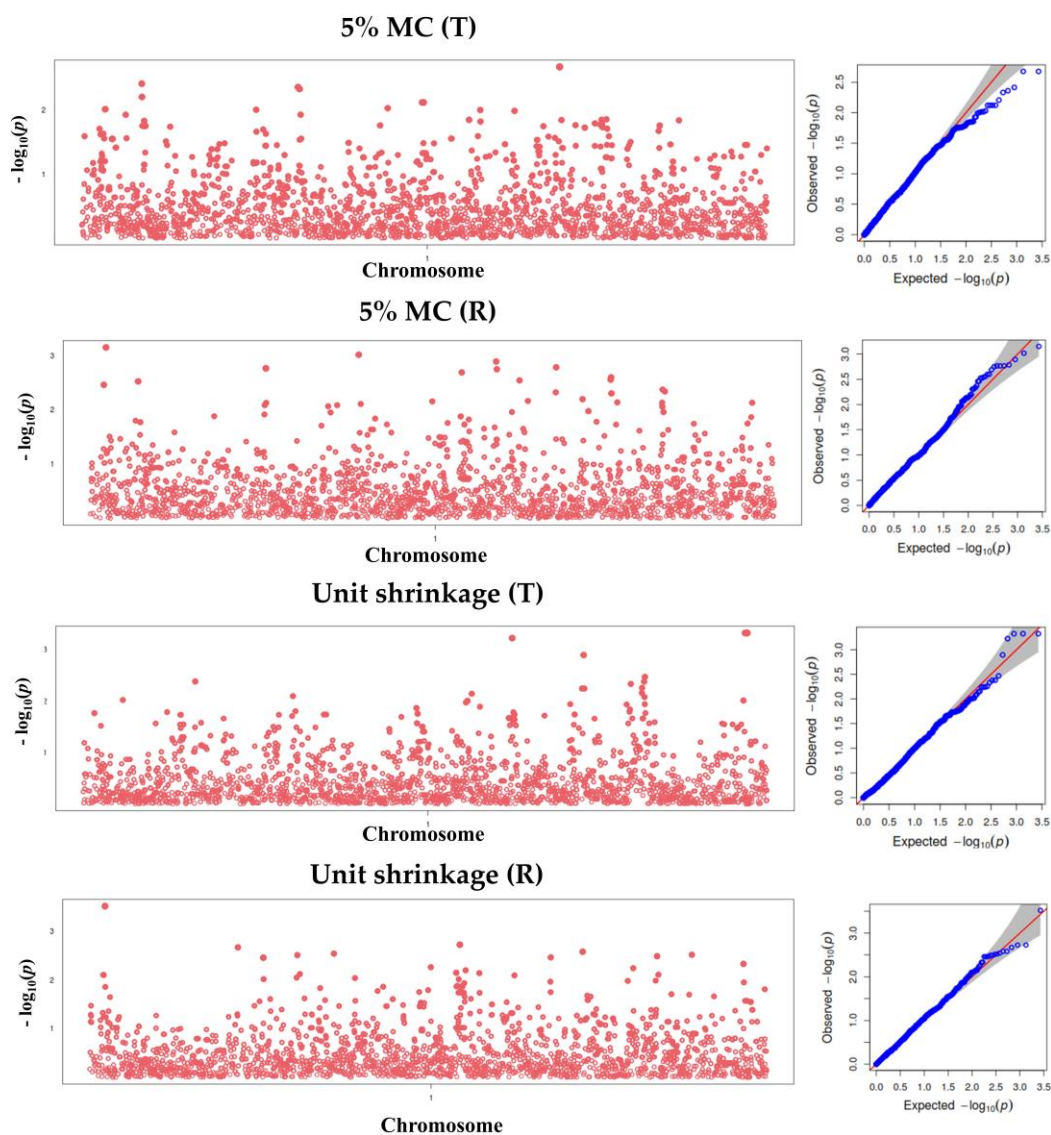


Figure 4. Manhattan and quantile-quantile (Q-Q) plots showing SNP associations with tangential (T) and radial (R) shrinkage at 5% MC, and unit shrinkage. In the Manhattan plots (left), each red dot represents an individual SNP, with its genomic position on the x-axis and the $-\log_{10}(p)$ value on the y-axis. In the Q-Q plots (right), blue dots represent observed p -values compared to the expected distribution under the null hypothesis. The red line indicates the expected distribution.

Given the number of SNP-trait comparisons conducted, the risk of false positives was addressed by applying the Benjamini–Hochberg false discovery rate (FDR) correction as implemented in the GAPIT analysis pipeline, with significance defined at an adjusted p -value < 0.05 . Of all the traits analyzed, only the SNPs associated with 12% AR (T) exceeded this corrected significance threshold (Figure 3), indicating a statistically robust association. Although several other SNPs had low nominal p -values (e.g., $p < 0.001$), they did not pass the threshold and are therefore considered suggestive. The Q-Q plots assess association reliability by comparing observed p -values to expected distributions. Most SNPs align with the expected trend, suggesting minimal confounding effects. However, deviations in 12% AR (T) reinforce its strong association, while green density (R) and oven-dry density (T and R) show weaker but potential genetic signals.

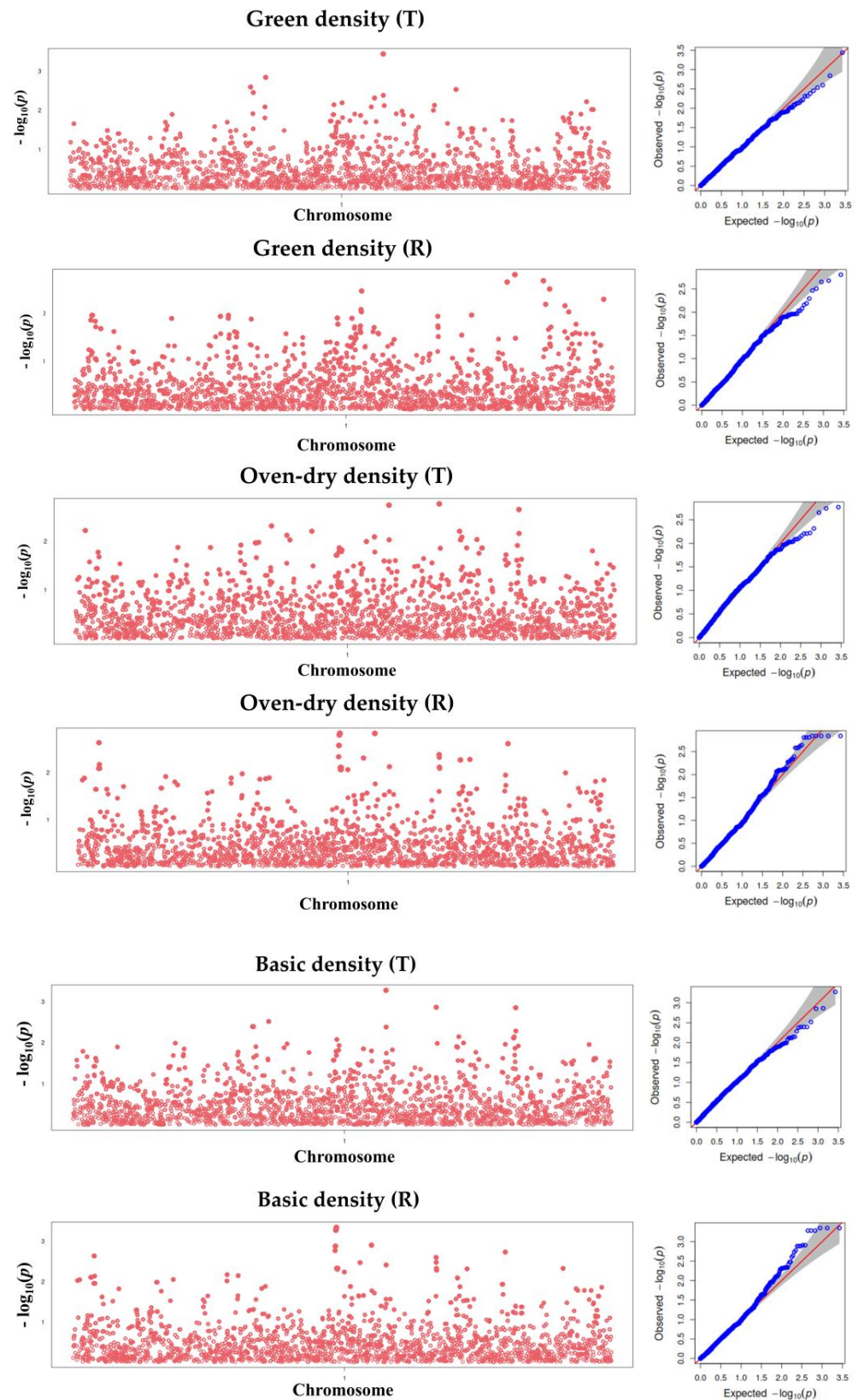


Figure 5. Manhattan and quantile-quantile (Q-Q) plots showing SNP associations with wood density traits (green density, oven-dry density, and basic density at the tangential (T) and radial (R) directions). In the Manhattan plots (left), each red dot represents an individual SNP, with its genomic position on the x-axis and the $-\log_{10}(p)$ value on the y-axis. In the Q-Q plots (right), blue dots represent observed p -values compared to the expected distribution under the null hypothesis. The red line indicates the expected distribution.

The combined analysis of Manhattan and Q-Q plots suggests that while many SNPs exhibit strong associations with shrinkage and density traits, only a limited number surpass the significance threshold. These preliminary findings point to potential genomic regions that may influence wood dimensional stability and density. However, the relatively small sample size in this study may limit statistical power, as previous studies with larger datasets have reported stronger associations [17,77,78]. For instance, Ballesta et al. [77] utilized a sample size of over 400 individuals to identify robust genetic associations with wood properties, while Tan and Ingvarsson [17] carried out their study on sample sizes exceeding 500 individuals. Given this limitation, the current results should be interpreted as exploratory, providing a basis for future studies with larger, well-replicated populations and multi-environment trials to enable more robust quantitative genetic analysis and multi-trait selection strategies.

3.5. Marker Identification for Wood Property Traits

The SNP-based genetic analysis was exploratory; given the modest sample size, it enabled the preliminary identification of SNPs potentially associated with shrinkage and density traits. These findings provide a foundation for future validation in larger and more diverse populations. Only SNP2554 for 12% AR (T) exceeded the significance threshold; however, the top five SNPs for each trait (based on the lowest p -values) were identified. SNPs that appeared in multiple traits are summarized in Tables 7 and 8. While these did not meet the strict threshold, they may still represent biological relevance given the small sample size and complex trait architecture. These findings provide a useful starting point for future validation and candidate gene exploration, though they should be interpreted with caution. Table 7 lists the SNPs associated with shrinkage traits, including their alleles, population structure positions (Pos), p -values ($p < 0.001$ and $p < 0.01$), minor allele frequency (MAF), allelic effects and the nearest gene. All significant SNPs identified were located on Chromosome 1, reflecting the design of the SNP panel developed by Gondwana Genomics, which targets this chromosome. Several SNPs were consistently linked to shrinkage and density across moisture levels and directions. SNP4963 was a key marker as it was associated with shrinkage at 17% MC, 12% BR, and unit shrinkage in the tangential direction ($p < 0.001$). SNP4976 and SNP4979 were also linked to these traits, both with $p < 0.001$, suggesting a role in dimensional stability (Table 7). In the radial direction, SNP1641 was associated with shrinkage at 12% BR ($p = 0.002$) and 12% AR ($p = 0.001$). SNP2256 also showed significant associations ($p = 0.002$ and $p < 0.001$). SNP117 was linked to shrinkage at 5% MC ($p < 0.001$) and unit shrinkage ($p < 0.001$).

For density traits, SNP2981 showed significant associations with green density ($p < 0.001$), oven-dry density ($p = 0.002$), and basic density ($p = 0.001$) in the tangential direction. SNP3459 and SNP4216 were also linked to oven-dry and basic density in the tangential direction. In the radial direction, SNP2507, SNP2508, and SNP2509 were the most significant markers for oven-dry density ($p = 0.001$) and basic density ($p < 0.001$) (Table 8). The presence of certain SNPs across multiple traits and directions suggests a broader influence on wood properties. For example, SNP4963 was associated with several shrinkage traits in the tangential direction. Similarly, SNP4976 and SNP4979 were linked to shrinkage at different moisture levels. SNP2981, SNP3459, and SNP4216 showed strong links to green density. Wood density affects mechanical properties and end-use applications [74,79]. These findings align with previous studies on genetic markers for wood density variations [80,81].

To better understand the potential biological functions of the significant SNPs, we conducted a functional annotation of nearby genes. Interestingly, all SNPs significantly associated with wood property traits in this study, including shrinkage at different moisture levels, unit shrinkage, green density, oven-dry density, and basic density, were located in the intergenic region near a single gene, *Eucgr.A00211*. These SNPs were annotated with a MODIFIER impact, suggesting potential regulatory functions without direct disruption of coding sequences. *Eucgr.A00211* encodes a lipase-containing protein related to the CGI-141 family (PTHR21493:SF110), which is implicated in lipid metabolism and membrane remodeling [82]. Although not directly involved in lignin or cellulose biosynthesis, lipase-related proteins have been linked to cell wall structure and dynamics [83], potentially influencing water transport, dimensional stability, and cell wall deposition processes. Given its predicted lipase activity, *Eucgr.A00211* may modulate lipid-mediated interactions between hemicellulose and lignin. Lignin and hemicelluloses form stable linkages via covalent and hydrogen bonds, which largely determine cell wall strength and water permeability [84]. Changes in the lipid environment may therefore alter the hydrophobicity or flexibility of the wall matrix, thereby influencing water retention and shrinkage behavior. These relationships are illustrated in a conceptual diagram (Figure 6), showing how *Eucgr.A00211* may influence cell wall properties and shrinkage behavior.

Table 7. Identified Single Nucleotide Polymorphisms (SNPs) associated with shrinkage traits at the Tangential (T) and Radial (R) directions, including the annotated gene information. All SNPs are located on Chromosome 1.

Marker Name	Shrinkage	Alleles	Pos	p-Value	MAF	Allelic Effect	Nearest Gene
SNP2554	Green to 12% AR (T)	T/C	2554	0.000 **	0.167	−2.303	<i>Eucgr.A00211</i>
SNP4979	Green to 17% MC (T)	A/C	4911	0.000 **	0.118	−1.996	
	Green to 12% MC BR (T)	A/C	4979	0.000 **	0.118	−1.888	
	Unit shrinkage (T)	A/C	4979	0.000 **	0.118	0.080	
SNP4963	Green to 17% MC (T)	T/A	4908	0.000 **	0.118	1.996	
	Green to 12% MC BR (T)	T/A	4963	0.000 **	0.118	1.888	
	Unit shrinkage (T)	T/A	4963	0.000 **	0.118	−0.080	
SNP4976	Green to 17% MC (T)	G/A	2975	0.000 **	0.118	1.996	
	Green to 12% MC BR (T)	G/A	4976	0.000 **	0.118	1.888	
	Unit shrinkage (T)	G/A	4976	0.000 **	0.118	−0.080	
SNP3575	Green to 12% MC BR (T)	C/T	3575	0.000 **	0.167	1.651	
	Green to 5% MC (T)	C/T	3575	0.002 *	0.167	1.053	
SNP3577	Green to 12% MC BR (T)	G/T	3577	0.000 **	0.167	1.651	
	Green to 5% MC (T)	G/T	3577	0.002 *	0.167	1.053	
SNP1123	Green to 12% MC BR (R)	C/T	1123	0.001 **	0.204	−1.112	
	Unit shrinkage (R)	C/T	1123	0.002 *	0.204	0.072	
SNP1641	Green to 12% MC BR (R)	C/G	1641	0.002 *	0.153	0.998	
	Green to 12% MC AR (R)	C/G	1641	0.001 **	0.153	1.010	
SNP2256	Green to 12% MC BR (R)	G/A	2256	0.002 *	0.122	0.922	
	Green to 12% MC AR (R)	G/A	2256	0.000 **	0.122	1.065	
SNP3769	Green to 12% MC BR (R)	A/G	3769	0.002 *	0.357	−0.702	
	Green to 12% MC AR (R)	A/G	3769	0.003 *	0.357	−0.675	

** $p < 0.001$, * $p < 0.01$; Pos: SNP position in the population structure; MAF: minor allele frequency; BR (Before reconditioning); AR (After reconditioning).

Table 8. Identified Single Nucleotide Polymorphisms (SNPs) associated with density traits at the Tangential (T) and Radial (R) directions, including the annotated gene information. All SNPs are located on Chromosome 1.

Marker Name	Density	Alleles	Pos	p-Value	MAF	Allelic Effect	Nearest Gene
SNP2981	Green density (T)	G/T	2981	0.000 **	0.098	69.245	<i>Eucgr.A00211</i>
	Basic density (T)	G/T	2981	0.001 **	0.098	70.362	
	Oven-dry density (T)	G/T	2981	0.002 *	0.098	78.225	
SNP1864	Green density (T)	G/A	1864	0.001 **	0.461	35.893	
	Oven-dry density (T)	G/A	1864	0.005 *	0.461	40.701	
	Basic density (T)	G/A	1864	0.003 *	0.461	34.975	
SNP3459	Oven-dry density (T)	G/A	3459	0.002 *	0.333	−46.823	
	Basic density (T)	G/A	3459	0.001 **	0.333	−39.114	
SNP4216	Oven-dry density (T)	A/T	4216	0.002 *	0.363	42.607	
	Basic density (T)	A/T	4216	0.001 **	0.363	36.333	
SNP2507	Oven-dry density (R)	T/C	2507	0.001 **	0.194	−62.993	
	Basic density (R)	T/C	2507	0.000 **	0.194	−56.888	
SNP2508	Oven-dry density (R)	T/C	2508	0.001 **	0.194	−62.993	
	Basic density (R)	T/C	2508	0.000 **	0.194	−56.888	
SNP2509	Oven-dry density (R)	T/C	2509	0.001 **	0.194	−62.993	
	Basic density (R)	T/C	2509	0.000 **	0.194	−56.888	

** $p < 0.001$, * $p < 0.01$, Chr: chromosomes; Pos: SNP position in the population structure; MAF: minor allele frequency.

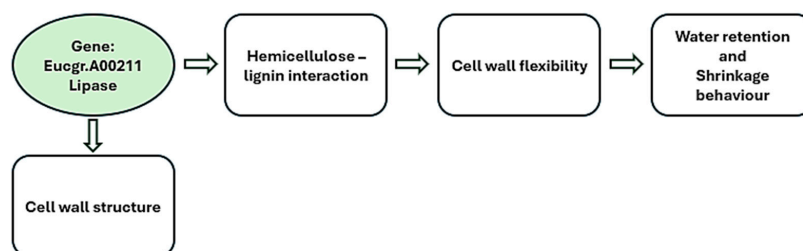


Figure 6. Conceptual diagram showing the potential role of *Eucgr.A00211* (lipase) in regulating cell wall structure and shrinkage behavior in *Eucalyptus pellita* hybrids.

In *E. grandis* and *E. urophylla*, Tan and Ingvarsson [17] used the GWAS approach and identified 49 candidate genes associated with wood traits, including those involved in cell wall biosynthesis and stress responses. Although the genomic regions differ from those identified in our study, both sets of findings point to regulatory genes, such as *Eucgr.A00211* in this study, as important contributors to variation in density and shrinkage through their influence on cell wall structure and water dynamics. The consistent association of SNPs near *Eucgr.A00211* across all examined traits in our study suggests a common genetic regulatory mechanism, possibly through transcriptional or post-transcriptional control of cell wall-related pathways. Given its broad relevance to key wood quality traits, SNPs near *Eucgr.A00211* represent promising candidates for marker-assisted selection in *Eucalyptus* breeding programs. However, functional validation, such as gene expression profiling or other molecular assays, is essential to confirm their regulatory role in cell wall dynamics and wood property variation.

Understanding the allelic effects of these SNPs is crucial for developing breeding strategies. A positive allelic effect increases the trait value, while a negative effect decreases it. For traits like shrinkage, where reduction is desirable, selecting alleles with negative effects can be beneficial. In industrial applications, tangential shrinkage exceeding 5% is linked to a higher incidence of warping, checking, and dimensional instability in solid

wood products [44]. Consequently, selecting genotypes with reduced shrinkage is critical for ensuring product performance during drying and in service. Similarly, basic wood density is a key determinant of end-use suitability. Medium to high-density ($> 500 \text{ kg/m}^3$) is generally preferred for structural and engineered wood applications due to their correlation with mechanical strength [85,86], whereas lower densities may be acceptable for pulp and paper production. By identifying SNPs with favorable allelic effects on these traits, such as reduced shrinkage or increased density, breeders can integrate molecular markers into marker-assisted selection (MAS) programs to accelerate genetic improvement [87]. This approach helps develop tree varieties with optimized wood properties, improving quality and performance.

Recent advances in forest tree genetics have greatly improved our understanding of the genetic architecture of wood properties in *Eucalyptus*. For instance, genomic prediction studies in *E. benthamii* have demonstrated that growth and wood density traits can be predicted with moderate to high accuracy using GBLUP, Bayesian ridge regression, and machine learning approaches, under varying SNP genotyping densities [88]. These findings highlight the potential of genomic tools to accelerate early selection for complex traits. Similarly, Duarte et al. [89] applied genomic selection across four generations of *E. grandis*, achieving realized genetic gains for growth and wood quality traits, thus demonstrating the long-term impact of SNP-based approaches in operational breeding programs.

Advancements in association mapping have also contributed significantly to dissecting complex traits. For example, cross-population GWAS (XP-GWAS), as applied by Giorello et al. [90] in *Eucalyptus*, increases detection power by leveraging allele frequency differences between populations. Although their study focused on leaf heteroblasty, the XP-GWAS approach shows strong potential for identifying adaptive loci associated with wood properties across heterogeneous plantation environments. This application is particularly relevant to *E. pellita* and its hybrids, which are frequently cultivated in environmentally diverse tropical regions. Additionally, recent GWAS in *E. grandis* employing both single- and multi-trait models have successfully detected QTLs for wood density, microfibril angle, and growth [91], reinforcing the polygenic basis of these traits and the value of multi-dimensional analysis frameworks.

While the relatively small sample size in this study may limit the detection of loci with minor effects, the repeated association of certain SNPs with shrinkage and density traits in *E. pellita* supports their potential biological relevance and provides a foundation for further research. These findings are consistent with the polygenic and site-dependent genetic control observed in related *Eucalyptus* species. To ensure their reliability and practical utility, these associations should be validated through cross-validation and testing in larger, independent populations across diverse environments. Incorporating mechanical properties alongside shrinkage and density in future studies will strengthen the application of marker-assisted selection and support the development of improved planting stock suitable for both structural and pulping applications.

4. Conclusions

This study integrated phenotypic and genomic data to assess variation in wood density and shrinkage among *Eucalyptus pellita* and its hybrids. Significant differences were observed among hybrid combinations, with *E. pellita* \times *E. urophylla* showing greater dimensional stability and *E. pellita* \times *E. brassiana* consistently exhibiting higher density. Strong correlations between physical traits, growth, and chemical composition indicate that wood properties are genetically influenced and may be indirectly selected through correlated traits, supporting more efficient breeding strategies. Hybrids with improved shrinkage performance, such as *E. pellita* \times *E. urophylla*, are promising for engineered

wood products where dimensional stability enhances processing and product performance. Conversely, the higher density in *E. pellita* × *E. brassiana* may benefit structural applications and increase pulp yield, aligning specific hybrid types with targeted industry uses.

The observed relationships among physical, growth, and chemical traits suggest that early selection based on productivity and chemical indicators may also capture desirable wood characteristics. These insights offer practical value to breeders aiming to streamline genotype development and improve resource use.

Although constrained by a relatively small sample size, the genetic analysis identified several SNPs associated with shrinkage and density traits, all located near a single gene (*Eucgr.A00211*), potentially involved in regulating wood cell structure and water retention. These findings provide early evidence of genetic control over wood physical traits and represent an initial step toward the use of molecular markers for trait-based selection in *Eucalyptus* breeding programs.

As this study focused on SNPs located on Chromosome 1, the findings offer insight into marker-trait associations within a limited genomic context. While this targeted approach may help reduce confounding variation and highlight strong signals, genome-wide screening could uncover additional loci associated with shrinkage, density, or related traits, particularly in more diverse or complex populations.

To advance these findings, future studies should validate Chromosome 1 SNP associations in larger, more diverse populations ($n > 300$) and across different environments. Including mechanical properties, such as modulus of elasticity, modulus of rupture, and compression strength, will further link wood traits to product functionality. Breeders can begin applying observed trait correlations, while industry stakeholders may align hybrid deployment with specific end-use goals to enhance material efficiency, support product diversification, and promote sustainable plantation forestry.

Author Contributions: Conceptualization, O.E.F., B.B., G.B., B.O., and A.S.; methodology, O.E.F. and B.B.; software, O.E.F.; validation, O.E.F., B.B., B.O., G.B., and A.S.; formal analysis, O.E.F.; investigation, O.E.F.; resources, B.B., B.O., A.S., and G.B.; data curation, O.E.F., L.M.D., U.I., and B.T.; writing—original draft preparation, O.E.F.; writing—review and editing, O.E.F., B.B., B.O., G.B., and A.S.; visualization, O.E.F.; supervision, B.B., A.S., B.O., and G.B.; project administration, O.E.F., B.B., G.B., and A.S.; funding acquisition, B.B., G.B., B.O., and A.S. All authors have read and agreed to the published version of the manuscript.

Funding: This research was funded by the Cooperative Research Centre for Developing Northern Australia (CRCNA) through the Australian Government CRC initiative, grant number: CN-00297, project number AT.4.2021001.

Data Availability Statement: The dataset is available on request from the authors.

Acknowledgments: The authors would like to thank the Tiwi Plantation Corporation (TPC), Midway, Gondwana Genomics, Forest and Wood Products Australia, Plantation Management Partners (PMP), the Northern Territory Government, and the Tiwi Land Council for their partnership in the project. We also appreciate Luke Austin (Southern Cross University) for his valuable assistance with tree harvesting and collection of materials used in this study.

Conflicts of Interest: The authors declare no conflicts of interest.

Appendix A

Tables A1 and A2 present the 95% confidence intervals for shrinkage and density values, respectively, among the *Eucalyptus* hybrids evaluated at Kilu Impini 64 (KI64), Yapilika 28 (YP28), and across the combined plantation sites. These intervals provide a statistical estimate of the variability and precision of the mean trait values, supporting the interpretation of site and hybrid effects reported in the main text.

Table A1. Confidence intervals for shrinkage values among hybrids at Kilu Impini 64 (KI64), Yapilika 28 (YP28), and combined plantation sites.

Plantation Sites/Hybrids	Green to 17% (%)		Green to 12% BR (%)		Green to 12% AR (%)		Green to 5% (%)		Unit Shrinkage (%)	
	T	R	T	R	T	R	T	R	T	R
KI64										
<i>E. pellita</i>	1.15–3.48	0.70–1.71	2.82–5.18	1.30–3.02	1.87–4.13	0.63–2.29	5.23–7.05	3.36–5.99	0.16–0.24	0.13–0.23
<i>E. pellita</i> × <i>E. brassiana</i> (BC)	2.55–5.16	0.99–2.21	3.98–6.56	1.67–3.75	3.07–5.62	1.33–3.34	5.70–7.65	2.99–6.17	0.15–0.23	0.09–0.21
<i>E. pellita</i> × <i>E. brassiana</i> (F1)	2.56–5.61	1.06–2.45	4.11–7.28	2.11–4.50	2.79–5.72	1.45–3.75	6.25–8.74	2.96–6.61	0.16–0.26	0.06–0.20
<i>E. pellita</i> × <i>E. urophylla</i> (BC)	1.21–3.44	1.03–1.95	2.82–5.09	2.17–3.74	1.89–4.04	1.26–2.77	4.87–6.64	2.89–5.29	0.15–0.23	0.08–0.18
<i>E. pellita</i> × <i>E. urophylla</i> (F1)	1.96–5.00	0.78–2.06	3.58–6.52	1.26–3.45	2.56–5.53	0.94–3.05	5.54–7.77	1.60–4.94	0.11–0.22	0.01–0.15
YP28										
<i>E. pellita</i>	1.13–2.90	1.07–1.77	2.68–4.39	2.02–3.11	2.08–3.63	1.58–2.68	5.32–6.76	3.70–5.68	0.19–0.23	0.09–0.20
<i>E. pellita</i> × <i>E. brassiana</i> (BC)	2.12–4.46	0.91–1.82	3.81–5.96	1.81–3.22	2.18–4.04	1.21–2.52	6.02–7.84	2.36–4.73	0.19–0.25	0.04–0.19
<i>E. pellita</i> × <i>E. brassiana</i> (F1)	5.20–8.46	2.55–3.47	6.48–9.65	3.51–4.92	5.67–8.51	3.18–4.49	7.37–10.04	3.37–5.75	0.07–0.15	0.01–0.16
<i>E. pellita</i> × <i>E. urophylla</i> (BC)	1.32–3.27	0.92–1.67	2.97–4.87	2.09–3.26	2.13–3.85	1.68–2.87	5.48–7.08	3.51–5.67	0.20–0.25	0.10–0.22
<i>E. pellita</i> × <i>E. urophylla</i> (F1)	2.47–4.79	0.74–2.39	3.78–5.99	1.18–3.71	2.96–4.92	0.83–3.44	5.54–7.41	2.47–7.22	0.14–0.19	0.05–0.31
Plantation sites combined										
<i>E. pellita</i>	1.58–2.74	0.73–1.93	3.12–4.35	1.75–3.01	2.30–3.56	1.21–2.51	5.35–6.70	3.90–5.30	0.17–0.24	0.13–0.19
<i>E. pellita</i> × <i>E. brassiana</i> (BC)	3.04–4.25	0.85–2.10	4.68–5.96	1.94–3.26	3.26–4.57	1.48–2.83	6.33–7.73	3.32–4.78	0.17–0.23	0.10–0.16
<i>E. pellita</i> × <i>E. brassiana</i> (F1)	4.39–5.92	1.72–2.93	5.73–7.38	3.08–4.35	4.51–6.17	2.49–3.80	7.11–8.90	3.94–5.34	0.15–9.23	0.08–0.15
<i>E. pellita</i> × <i>E. urophylla</i> (BC)	1.74–2.94	0.82–2.02	3.33–4.59	2.22–3.49	2.37–3.67	1.52–2.82	5.33–6.73	3.70–5.10	0.17–0.24	0.11–0.17
<i>E. pellita</i> × <i>E. urophylla</i> (F1)	2.88–4.15	0.30–2.00	4.17–5.52	1.22–3.05	3.38–4.76	0.89–2.73	5.75–7.23	2.41–4.40	0.13–0.20	0.06–0.15

F1: first-generation hybrid; BC: backcross; BR: Before reconditioning; AR: After reconditioning; T: Tangential; R: Radial. Level of significance ($p < 0.05$), Confidence level used = 0.95.

Table A2. Confidence intervals for density values among hybrids at Kilu Impini 64 (KI64), Yapilika 28 (YP28), and combined plantation sites.

Plantation Sites/Hybrids	Green Density (kg/m ³)		Oven-Dry Density (kg/m ³)		Basic Density (kg/m ³)	
	T	R	T	R	T	R
KI64						
<i>E. pellita</i>	1034.00–1135.00	1010.00–1079.00	631.00–771.00	529.00–649.00	537.00–648.00	480.00–583.00
<i>E. pellita</i> × <i>E. brassiana</i> (BC)	1103.00–1210.00	1044.00–1127.00	694.00–838.00	579.00–716.00	585.00–701.00	514.00–631.00
<i>E. pellita</i> × <i>E. brassiana</i> (F1)	1067.00–1206.00	1043.00–1138.00	683.00–879.00	549.00–703.00	550.00–705.00	487.00–618.00
<i>E. pellita</i> × <i>E. urophylla</i> (BC)	1038.00–1137.00	1026.00–1089.00	625.00–766.00	532.00–641.00	533.00–644.00	487.00–581.00
<i>E. pellita</i> × <i>E. urophylla</i> (F1)	1032.00–1154.00	1025.00–1113.00	610.00–776.00	527.00–683.00	505.00–638.00	478.00–612.00

Table A2. Cont.

Plantation Sites/Hybrids	Green Density (kg/m ³)		Oven-Dry Density (kg/m ³)		Basic Density (kg/m ³)	
	T	R	T	R	T	R
YP28						
<i>E. pellita</i>	1056.00–1150.00	1000.00–1083.00	621.00–743.00	531.00–633.00	533.00–625.00	484.00–568.00
<i>E. pellita</i> × <i>E. brassiana</i> (BC)	1105.00–1206.00	1064.00–1164.00	694.00–835.00	610.00–736.00	583.00–694.00	547.00–651.00
<i>E. pellita</i> × <i>E. brassiana</i> (F1)	1031.00–1185.00	1015.00–1115.00	634.00–851.00	569.00–694.00	512.00–681.00	499.00–603.00
<i>E. pellita</i> × <i>E. urophylla</i> (BC)	1071.00–1170.00	1011.00–1102.00	683.00–816.00	564.00–675.00	569.00–671.00	506.00–597.00
<i>E. pellita</i> × <i>E. urophylla</i> (F1)	1063.00–1170.00	1005.00–1204.00	641.00–790.00	542.00–784.00	547.00–664.00	492.00–691.00
Plantation sites combined						
<i>E. pellita</i>	1062.00–1119.00	1008.00–1068.00	645.00–725.00	542.00–624.00	551.00–614.00	495.00–559.00
<i>E. pellita</i> × <i>E. brassiana</i> (BC)	1132.00–1192.00	1072.00–1134.00	746.00–830.00	624.00–709.00	618.00–684.00	558.00–625.00
<i>E. pellita</i> × <i>E. brassiana</i> (F1)	1097.00–1172.00	1054.00–1114.00	716.00–812.00	586.00–670.00	576.00–653.00	519.00–584.00
<i>E. pellita</i> × <i>E. urophylla</i> (BC)	1080.00–1139.00	1027.00–1087.00	679.00–772.00	558.00–650.00	571.00–643.00	507.00–580.00
<i>E. pellita</i> × <i>E. urophylla</i> (F1)	1092.00–1156.00	1041.00–1123.00	692.00–780.00	575.00–679.00	577.00–646.00	522.00–606.00

F1: first-generation hybrid; BC: backcross; T: Tangential; R: Radial. Level of significance ($p < 0.05$), Confidence level used = 0.95.

References

1. Rhodes, D.; Stephens, M. Planted Forest Development in Australia and New Zealand: Comparative Trends and Future Opportunities. *N. Z. J. For. Sci.* **2014**, *44*, S10. [\[CrossRef\]](#)
2. Lindenmayer, D.; Taylor, C. Diversifying Forest Landscape Management—A Case Study of a Shift from Native Forest Logging to Plantations in Australian Wet Forests. *Land* **2022**, *11*, 407. [\[CrossRef\]](#)
3. Downham, R.; Gavran, M. *Australian Plantation Statistics 2020 Update*; Australian Bureau of Agricultural and Resource Economics and Sciences (ABARES): Canberra, Australia, 2020; p. 21.
4. McGavin, R.L.; Leggate, W. Comparison of Processing Methods for Small-Diameter Logs: Sawing Versus Rotary Peeling. *BioResources* **2019**, *14*, 1545–1563. [\[CrossRef\]](#)
5. Pliura, A.; Yu, Q.; Zhang, S.Y.; MacKay, J.; Périnet, P.; Bousquet, J. Variation in Wood Density and Shrinkage and Their Relationship to Growth of Selected Young Poplar Hybrid Crosses. *For. Sci.* **2005**, *51*, 472–482. [\[CrossRef\]](#)
6. Sargent, R. Evaluating Dimensional Stability in Solid Wood: A Review of Current Practice. *J. Wood Sci.* **2019**, *65*, 36. [\[CrossRef\]](#)
7. Japarudin, Y.; Meder, R.; Lapammu, M.; Waburton, P.; Paul-Macdonell, P.; Brown, M.; Brawner, J. Developing *Eucalyptus pellita* Breeding Populations for the Solid Wood Industry of Eastern Malaysia. *J. Trop. For. Sci.* **2022**, *34*, 347–358. [\[CrossRef\]](#)
8. Japarudin, Y.; Lapammu, M.; Alwi, A.; Warburton, P.; Macdonell, P.; Boden, D.; Brawner, J.; Brown, M.; Meder, R. Growth Performance of Selected Taxa as Candidate Species for Productive Tree Plantations in Borneo. *Aust. For.* **2020**, *83*, 29–38. [\[CrossRef\]](#)
9. de Oliveira Castro, C.A.; dos Santos, G.A.; Takahashi, E.K.; Pires Nunes, A.C.; Souza, G.A.; de Resende, M.D.V. Accelerating *Eucalyptus* Breeding Strategies through Top Grafting Applied to Young Seedlings. *Ind. Crops Prod.* **2021**, *171*, 113906. [\[CrossRef\]](#)
10. Muneera Parveen, A.B.; Muthupandi, M.; Kumar, N.; Chauhan, S.S.; Vellaichamy, P.; Senthamilselvam, S.; Rajasugunasekar, D.; Nagarajan, B.; Mayavel, A.; Bachpai, V.K.W.; et al. Quantitative Genetic Analysis of Wood Property Traits in Biparental Population of *Eucalyptus camaldulensis* × *E. tereticornis*. *J. Genet.* **2021**, *100*, 46. [\[CrossRef\]](#) [\[PubMed\]](#)
11. Simiqueli, G.F.; Resende, R.T.; Takahashi, E.K.; de Sousa, J.E.; Grattapaglia, D. Realized Genomic Selection across Generations in a Reciprocal Recurrent Selection Breeding Program of *Eucalyptus* Hybrids. *Front. Plant Sci.* **2023**, *14*, 1252504. [\[CrossRef\]](#)
12. Prasetyo, A.; Aiso-Sanada, H.; Ishiguri, F.; Wahyudi, I.; Wijaya, I.P.G.; Ohshima, J.; Yokota, S. Growth Characteristics and Wood Properties of Two Interspecific *Eucalyptus* Hybrids Developed in Indonesia. *For. Prod. J.* **2018**, *68*, 436–444. [\[CrossRef\]](#)
13. Van Duong, D.; Hasegawa, M.; Yamauchi, S.; Do, C.H. Within-Tree Variation Regarding Ultrasonic Velocity, Wood Density and Compressive Strength of the Eucalypt Hybrid (*Eucalyptus urophylla* × *E. pellita*). *Wood Mater. Sci. Eng.* **2024**, *20*, 420–426. [\[CrossRef\]](#)
14. Ramage, M.H.; Burrridge, H.; Busse-Wicher, M.; Fereday, G.; Reynolds, T.; Shah, D.U.; Wu, G.; Yu, L.; Fleming, P.; Densley-Tingley, D.; et al. The Wood from the Trees: The Use of Timber in Construction. *Renew. Sustain. Energy Rev.* **2017**, *68*, 333–359. [\[CrossRef\]](#)
15. Hassan Vand, M.; Tippner, J.; Brabec, M. Effects of Species and Moisture Content on the Behaviour of Solid Wood under Impact. *Eur. J. Wood Wood Prod.* **2024**, *82*, 23–34. [\[CrossRef\]](#)
16. Teodorescu, I.; Erbasu, R.; Branco, J.M.; Tăpuși, D. Study in the Changes of the Moisture Content in Wood. *IOP Conf. Ser. Earth Environ. Sci.* **2021**, *664*, 012017. [\[CrossRef\]](#)
17. Tan, B.; Ingvarsson, P.K. Integrating Genome-Wide Association Mapping of Additive and Dominance Genetic Effects to Improve Genomic Prediction Accuracy in *Eucalyptus*. *Plant Genome* **2022**, *15*, e20208. [\[CrossRef\]](#) [\[PubMed\]](#)
18. Gion, J.-M.; Carouché, A.; Deweer, S.; Bedon, F.; Pichavant, F.; Charpentier, J.-P.; Baillères, H.; Rozenberg, P.; Carocha, V.; Ognouabi, N.; et al. Comprehensive Genetic Dissection of Wood Properties in a Widely-Grown Tropical Tree: *Eucalyptus*. *BMC Genom.* **2011**, *12*, 301. [\[CrossRef\]](#) [\[PubMed\]](#)
19. Huang, C.-L.; Lindström, H.; Nakada, R.; Ralston, J. Cell Wall Structure and Wood Properties Determined by Acoustics—A Selective Review. *Holz Als Roh-Und Werkst.* **2003**, *61*, 321–335. [\[CrossRef\]](#)
20. Wang, X.; Zhao, W.; Zhang, Y.; Shi, J.; Shan, S.; Cai, L. Exploring Wood Micromechanical Structure: Impact of Microfibril Angle and Crystallinity on Cell Wall Strength. *J. Build. Eng.* **2024**, *90*, 109452. [\[CrossRef\]](#)
21. Hamilton, M.G.; Potts, B.M.; Greaves, B.L.; Dutkowski, G.W. Genetic Correlations between Pulpwood and Solid-Wood Selection and Objective Traits in *Eucalyptus globulus*. *Ann. For. Sci.* **2010**, *67*, 511. [\[CrossRef\]](#)
22. Nickolas, H.; Williams, D.; Downes, G.; Tilyard, P.; Harrison, P.A.; Vaillancourt, R.E.; Potts, B. Genetic Correlations among Pulpwood and Solid-Wood Selection Traits in *Eucalyptus globulus*. *New For.* **2020**, *51*, 137–158. [\[CrossRef\]](#)
23. Ho, T.X.; Schimleck, L.R.; Sinha, A. Utilization of Genetic Algorithms to Optimize *Eucalyptus globulus* Pulp Yield Models Based on Nir Spectra. *Wood Sci. Technol.* **2021**, *55*, 757–776. [\[CrossRef\]](#)
24. Kombi Kaviriri, D.; Liu, H.; Zhao, X. Estimation of Genetic Parameters and Wood Yield Selection Index in a Clonal Trial of Korean Pine (*Pinus koraiensis*) in Northeastern China. *Sustainability* **2021**, *13*, 4167. [\[CrossRef\]](#)
25. Nayanathara, R.M.O.; Leng, W.; Street, J.; Zhang, X. Wood Dimensional Stability Enhancement by Multivalent Metal-Cation-Induced Lignocellulosic Microfibrils Crosslinking. *Int. J. Biol. Macromol.* **2024**, *269*, 131877. [\[CrossRef\]](#) [\[PubMed\]](#)

26. Climent, J.; Alía, R.; Karkkainen, K.; Bastien, C.; Benito-Garzon, M.; Bouffier, L.; De Dato, G.; Delzon, S.; Dowkiw, A.; Elvira-Recuenco, M.; et al. Trade-Offs and Trait Integration in Tree Phenotypes: Consequences for the Sustainable Use of Genetic Resources. *Curr. For. Rep.* **2024**, *10*, 196–222. [\[CrossRef\]](#)
27. Jurcic, E.J.; Villalba, P.V.; Dutour, J.; Centurión, C.; Munilla, S.; Cappa, E.P. Breeding Value Predictive Accuracy for Scarcely Recorded Traits in a *Eucalyptus grandis* Breeding Population Using Genomic Selection and Data on Predictor Traits. *Tree Genet. Genomes* **2023**, *19*, 35. [\[CrossRef\]](#)
28. Marco de Lima, B.; Cappa, E.P.; Silva-Junior, O.B.; Garcia, C.; Mansfield, S.D.; Grattapaglia, D. Quantitative Genetic Parameters for Growth and Wood Properties in *Eucalyptus “Urograndis”* Hybrid Using near-Infrared Phenotyping and Genome-Wide Snp-Based Relationships. *PLoS ONE* **2019**, *14*, e0218747. [\[CrossRef\]](#) [\[PubMed\]](#)
29. Pan, Y.; Jiang, L.; Xu, G.; Li, J.; Wang, B.; Li, Y.; Zhao, X. Evaluation and Selection Analyses of 60 *Larix Kaempferi* Clones in Four Provenances Based on Growth Traits and Wood Properties. *Tree Genet. Genomes* **2020**, *16*, 1–11. [\[CrossRef\]](#)
30. Sargent, R. Evaluating Dimensional Stability in Modified Wood: An Experimental Comparison of Test Methods. *Forests* **2022**, *13*, 613. [\[CrossRef\]](#)
31. Shen, X.; Yang, S.; Li, G.; Liu, S.; Chu, F. The Contribution Mechanism of Furfuryl Alcohol Treatment on the Dimensional Stability of Plantation Wood. *Ind. Crops Prod.* **2022**, *186*, 115143. [\[CrossRef\]](#)
32. Owoyemi, J.M.; Falade, O.E.; Iyiola, E.A.; Oladapo, O.D. An Analysis of Impact of Furfurylation Treatments on the Physical and Mechanical Properties of *Pterygota macrocarpa* Wood. *J. Mater. Sci. Res. Rev.* **2023**, *6*, 6–23.
33. Cao, Y.; Li, X.; Liu, L.; Xie, G.; Lai, M.; Gao, J. Increased Dimensional Stability of *Eucalyptus grandis* × *Eucalyptus urophylla* ‘Glu9’ Wood through Palm Oil Thermal Treatment. *BioResources* **2023**, *18*, 3471–3478. [\[CrossRef\]](#)
34. He, L.; Zhang, T.; Zhao, Y.; Gao, J.; Zhang, Y.; Yang, Y.; He, Z.; Yi, S. Effect of Natural Tung Oil on Wood Shrinkage During the Thermal Modification Process. *J. Clean. Prod.* **2022**, *379*, 134450. [\[CrossRef\]](#)
35. Tibbits, J.F.G.; McManus, L.J.; Spokevicius, A.V.; Bossinger, G. A Rapid Method for Tissue Collection and High-Throughput Isolation of Genomic DNA from Mature Trees. *Plant Mol. Biol. Rep.* **2006**, *24*, 81–91. [\[CrossRef\]](#)
36. Kingston, R.S.T.; Risdon, C.J.E. *Shrinkage and Density of Australian and Other South-West Pacific Woods*; Commonwealth Scientific and Industrial Research Organization: Melbourne, VIC, Australia, 1961; pp. 1–23.
37. ASTM D2395-17; Standard Test Methods for Density and Specific Gravity (Relative Density) of Wood and Wood-Based Materials. ASTM: West Conshohocken, PA, USA, 2017.
38. Poke, F.S.; Raymond, C.A. Predicting Extractives, Lignin, and Cellulose Contents Using near Infrared Spectroscopy on Solid Wood in *Eucalyptus globulus*. *J. Wood Chem. Technol.* **2006**, *26*, 187–199. [\[CrossRef\]](#)
39. Downes, G.M.; Meder, R.; Bond, H.; Ebdon, N.; Hicks, C.; Harwood, C. Measurement of Cellulose Content, Kraft Pulp Yield and Basic Density in Eucalypt Woodmeal Using Multisite and Multispecies near Infra-Red Spectroscopic Calibrations. *South. For.* **2011**, *73*, 181–186. [\[CrossRef\]](#)
40. Gondwana Genomics. Maximise Your Growth, Density, Pulp Yield. Available online: <https://gondwanagenomics.com.au/> (accessed on 24 May 2025).
41. Tang, Y.; Liu, X.; Wang, J.; Li, M.; Wang, Q.; Tian, F.; Su, Z.; Pan, Y.; Liu, D.; Lipka, A.E.; et al. Gapit Version 2: An Enhanced Integrated Tool for Genomic Association and Prediction. *Plant Genome* **2016**, *9*, plantgenome2015.2011.0120. [\[CrossRef\]](#)
42. Huang, M.; Liu, X.; Zhou, Y.; Summers, R.M.; Zhang, Z. Blink: A Package for the Next Level of Genome-Wide Association Studies with Both Individuals and Markers in the Millions. *GigaScience* **2018**, *8*, 1–12. [\[CrossRef\]](#) [\[PubMed\]](#)
43. Benjamini, Y.; Hochberg, Y. Controlling the False Discovery Rate: A Practical and Powerful Approach to Multiple Testing. *J. R. Stat. Soc. Ser. B Methodol.* **1995**, *57*, 289–300. [\[CrossRef\]](#)
44. Gao, Y.; Fu, Z.; Zhou, Y.; Gao, X.; Zhou, F.; Cao, H. Moisture-Related Shrinkage Behavior of Wood at Macroscale and Cellular Level. *Polymers* **2022**, *14*, 5045. [\[CrossRef\]](#) [\[PubMed\]](#)
45. Gezici-Koç, Ö.; Erich, S.J.F.; Huinink, H.P.; van der Ven, L.G.J.; Adan, O.C.G. Bound and Free Water Distribution in Wood During Water Uptake and Drying as Measured by 1d Magnetic Resonance Imaging. *Cellulose* **2017**, *24*, 535–553. [\[CrossRef\]](#)
46. Baillères, H.; Hopewell, G.; McGavin, R.L. *Evaluation of Wood Characteristics of Tropical Post-Mid Rotation Plantation Eucalyptus cloeziana and E. pellita: Part (C) Wood Quality and Structural Properties*; PN07.3022; Forest & Wood Product Australia: Melbourne, VIC, Australia, 2008.
47. WoodSolutions. Mahogany, Red—Overview. Available online: <https://www.woodsolutions.com.au/wood-species/hardwood/mahogany-red> (accessed on 10 November 2023).
48. Sattar, M.A.; Bhattacharjee, D.K.; Kabir, M.F. *Physical and Mechanical Properties and Uses of Timbers of Bangladesh*; Bangladesh Forest Research Institute: Chittagong, Bangladesh; Government of the People’s Republic of Bangladesh: Dhaka, Bangladesh, 1999; pp. 1–57.
49. Kabir, M.F.; Sattar, M.A. Strength Properties and Drying Characteristics of *Eucalyptus* Wood Grown in Bangladesh. *Thai J. For.* **1995**, *14*, 103–109.
50. Júnior, L.S.; Garcia, J.N. Physical and Mechanical Properties of *Eucalyptus urophylla*. *Braz. J. Agric.* **2023**, *98*, 12–22. [\[CrossRef\]](#)

51. Wu, Y.-Q.; Hayashi, K.; Liu, Y.; Cai, Y.; Sugimori, M. Relationships of Anatomical Characteristics Versus Shrinkage and Collapse Properties in Plantation-Grown Eucalypt Wood from China. *J. Wood Sci.* **2006**, *52*, 187–194. [\[CrossRef\]](#)
52. Thomson, A.B. *Shrinkage, Collapse and Dimensional Recovery of Regrowth Jarrah*; Wood Utilisation Reserach Centre: Kensington, WA, Australia, 1989; pp. 1–11.
53. Yang, L.; Liu, H. A Review of *Eucalyptus* Wood Collapse and Its Control During Drying. *BioResources* **2018**, *13*, 2171–2181. [\[CrossRef\]](#)
54. Gonya, N.A.S.; Naghizadeh, Z.; Wessels, C.B. An Investigation into Collapse and Shrinkage Behaviour of *Eucalyptus grandis* and *Eucalyptus grandis-urophylla* Wood. *Eur. J. Wood Wood Prod.* **2022**, *80*, 139–157. [\[CrossRef\]](#)
55. Blakemore, P.; Langrish, T.A.G. Effect of Mean Moisture Content on the Steam Reconditioning of Collapsed *Eucalyptus regnans*. *Wood Sci. Technol.* **2007**, *41*, 87–98. [\[CrossRef\]](#)
56. Ibarra, L.; Hodge, G.; Acosta, J.J. Quantitative Genetics of a Hybrid Population of *Eucalyptus nitens* × *Eucalyptus globulus*: Estimation of Genetic Parameters and Implications for Breeding Strategies. *Forests* **2023**, *14*, 381. [\[CrossRef\]](#)
57. Parveen, A.B.M.; Jayabharathi, K.; Muthupandi, M.; Kumar, N.; Chauhan, S.S.; Rajasugunasekar, D.; Dasgupta, M.G. Identification of Superior Hybrid Clones for Fibre Biometry in *Eucalyptus camaldulensis* × *E. tereticornis* Using Multi Trait Stability Index. *Silvae Genet.* **2024**, *73*, 126–141. [\[CrossRef\]](#)
58. Japarudin, Y.; Meder, R.; Lapammu, M.; Alwi, A.; Ghaffariyan, M.; Brown, M. Compression and Flexural Properties of Plantation-Grown *Eucalyptus pellita* in Borneo, Malaysia. Potential for Structural Timber End Use. *Aust. For.* **2021**, *84*, 139–151. [\[CrossRef\]](#)
59. Hii, S.Y.; Ha, K.S.; Ngui, M.L.; Ak Penguang, S.; Duju, A.; Teng, X.Y.; Meder, R. Assessment of Plantation-Grown *Eucalyptus pellita* in Borneo, Malaysia for Solid Wood Utilisation. *Aust. For.* **2017**, *80*, 26–33. [\[CrossRef\]](#)
60. Bergman, R. Drying and Control of Moisture Content and Dimensional Changes. In *Wood Handbook*; U.S. Department of Agriculture: Washington, DC, USA, 2021; pp. 1–21.
61. Li, F.; Qian, H.; Sardans, J.; Amishev, D.Y.; Wang, Z.; Zhang, C.; Wu, T.; Xu, X.; Tao, X.; Huang, X. Evolutionary History Shapes Variation of Wood Density of Tree Species across the World. *Plant Divers.* **2024**, *46*, 283–293. [\[CrossRef\]](#)
62. Downes, G.M.; Lausberg, M.; Potts, B.M.; Pilbeam, D.L.; Bird, M.; Bradshaw, B. Application of the Iml Resistograph to the Infield Assessment of Basic Density in Plantation Eucalypts. *Aust. For.* **2018**, *81*, 177–185. [\[CrossRef\]](#)
63. Drew, D.M.; Downes, G.M.; Seifert, T.; Eckes-Shepard, A.; Achim, A. A Review of Progress and Applications in Wood Quality Modelling. *Curr. For. Rep.* **2022**, *8*, 317–332. [\[CrossRef\]](#)
64. Elissetche, J.P.; Alzamora, R.M.; Espinoza, Y.; Emhart, V.; Pincheira, M.; Medina, A.; Rubilar, R. Wood Basic Density Assessment of *Eucalyptus* Genotypes Growing under Contrasting Water Availability Conditions. *Forests* **2024**, *15*, 185. [\[CrossRef\]](#)
65. Schulgasser, K.; Witztum, A. How the Relationship between Density and Shrinkage of Wood Depends on Its Microstructure. *Wood Sci. Technol.* **2015**, *49*, 389–401. [\[CrossRef\]](#)
66. Pulgar, J.A.; Riesco, G. Implementing Linear Mixed Effects Models to Enhance Estimation of the Dimensional Stability of Wood of *Laurus nobilis* L. *For. Syst.* **2024**, *33*, e05. [\[CrossRef\]](#)
67. Listyanto, T.; Nichols, J.D.; Glencross, K.; Schoer, L. Variation in Density and Shrinkage of Six *Eucalyptus* Species and Interspecific Hybrid Combinations at Three Sites in Northern New South Wales. *IOP Conf. Ser. Mater. Sci. Eng.* **2020**, *935*, 012035. [\[CrossRef\]](#)
68. Lachenbruch, B.; Moore, J.; Evans, R. Radial Variation in Wood Structure and Function in Woody Plants, and Hypotheses for Its Occurrence. In *Size- and Age-Related Changes in Tree Structure and Function*; Springer: Dordrecht, The Netherlands, 2011; Volume 4, pp. 121–164.
69. Xiang, W.; Leitch, M.; Auty, D.; Duchateau, E.; Achim, A. Radial Trends in Black Spruce Wood Density Can Show an Age- and Growth-Related Decline. *Ann. For. Sci.* **2014**, *71*, 603–615. [\[CrossRef\]](#)
70. Dhaka, R.K.; Gunaga, R.P.; Sinha, S.K.; Thakur, N.S.; Dobriyal, M.J. Influence of Tree Height and Diameter on Wood Basic Density, Cellulose and Fibre Characteristics in *Melia Dubia* Cav. Families. *J. Indian Acad. Wood Sci.* **2020**, *17*, 138–144. [\[CrossRef\]](#)
71. Rocha, M.F.V.; Veiga, T.R.L.A.; Soares, B.C.D.; Araújo, A.C.C.d.; Carvalho, A.M.M.; Hein, P.R.G. Do the Growing Conditions of Trees Influence the Wood Properties? *Floresta E Ambient.* **2019**, *26*, e20180353. [\[CrossRef\]](#)
72. Kumar, A.; Jyske, T.; Petrič, M. Delignified Wood from Understanding the Hierarchically Aligned Cellulosic Structures to Creating Novel Functional Materials: A Review. *Adv. Sustain. Syst.* **2021**, *5*, 2000251. [\[CrossRef\]](#)
73. Azmul Huda, A.S.M.; Koubaa, A.; Cloutier, A.; Hernandez, R.E.; Perinet, P.; Fortin, Y. Phenotypic and Genotypic Correlations for Wood Properties of Hybrid Poplar Clones of Southern Quebec. *Forests* **2018**, *9*, 140. [\[CrossRef\]](#)
74. Zhang, S.Y.; Ren, H.; Jiang, Z. Wood Density and Wood Shrinkage in Relation to Initial Spacing and Tree Growth in Black Spruce (*Picea mariana*). *J. Wood Sci.* **2021**, *67*, 30. [\[CrossRef\]](#)
75. Gierlinger, N. New Insights into Plant Cell Walls by Vibrational Microspectroscopy. *Appl. Spectrosc. Rev.* **2018**, *53*, 517–551. [\[CrossRef\]](#)
76. Kocaefe, D.; Huang, X.; Kocaefe, Y. Dimensional Stabilization of Wood. *Curr. For. Rep.* **2015**, *1*, 151–161. [\[CrossRef\]](#)
77. Ballesta, P.; Bush, D.; Silva, F.F.; Mora, F. Genomic Predictions Using Low-Density Snp Markers, Pedigree and Gwas Information: A Case Study with the Non-Model Species *Eucalyptus cladocalyx*. *Plants* **2020**, *9*, 99. [\[CrossRef\]](#) [\[PubMed\]](#)

78. Wang, C.; Lan, J.; Wang, J.; He, W.; Lu, W.; Lin, Y.; Luo, J. Population Structure and Genetic Diversity in *Eucalyptus pellita* Based on Snp Markers. *Front. Plant Sci.* **2023**, *14*, 1278427. [[CrossRef](#)] [[PubMed](#)]
79. Lehnebach, R.; Bossu, J.; Va, S.; Morel, H.; Amusant, N.; Nicolini, E.; Beauchêne, J. Wood Density Variations of Legume Trees in French Guiana Along the Shade Tolerance Continuum: Heartwood Effects on Radial Patterns and Gradients. *Forests* **2019**, *10*, 80. [[CrossRef](#)]
80. Raymond, C.A. Genetics of *Eucalyptus* Wood Properties. *Ann. For. Sci.* **2002**, *59*, 525–531. [[CrossRef](#)]
81. Bano, N.; Mohammad, N.; Ansari, M.I.; Ansari, S.A. Discovery of Snps in Lignin Biosynthesis Genes (Cad1, Myb1 and Myb2) and Their Association with Wood Density in Teak. *Res. Sq.* **2023**. [[CrossRef](#)]
82. Li-Beisson, Y.; Shorosh, B.; Beisson, F.; Andersson, M.X.; Arondel, V.; Bates, P.D.; Baud, S.; Bird, D.; DeBono, A.; Durrett, T.P.; et al. Acyl-Lipid Metabolism. *Arab. Book* **2013**, *11*, e0161. [[CrossRef](#)] [[PubMed](#)]
83. Yan, X.; Ma, L.; Yang, M. Identification and Characterization of Long Non-Coding Rna (Lncrna) in the Developing Seeds of *Jatropha curcas*. *Sci. Rep.* **2020**, *10*, 10395. [[CrossRef](#)]
84. Terrett, O.M.; Dupree, P. Covalent Interactions between Lignin and Hemicelluloses in Plant Secondary Cell Walls. *Curr. Opin. Biotechnol.* **2019**, *56*, 97–104. [[CrossRef](#)]
85. Kovryga, A.; Stapel, P.; van de Kuilen, J.W.G. Mechanical Properties and Their Interrelationships for Medium-Density European Hardwoods, Focusing on Ash and Beech. *Wood Mater. Sci. Eng.* **2020**, *15*, 289–302. [[CrossRef](#)]
86. Nenning, T.; Tockner, A.; Konnerth, J.; Gindl-Altmutter, W.; Grabner, M.; Hansmann, C.; Lux, S.; Pramreiter, M. Variability of Mechanical Properties of Hardwood Branches According to Their Position and Inclination in the Tree. *Constr. Build. Mater.* **2024**, *419*, 135448. [[CrossRef](#)]
87. Du, Q.; Lu, W.; Quan, M.; Xiao, L.; Song, F.; Li, P.; Zhou, D.; Xie, J.; Wang, L.; Zhang, D. Genome-Wide Association Studies to Improve Wood Properties: Challenges and Prospects. *Front. Plant Sci.* **2018**, *9*, 1912. [[CrossRef](#)]
88. Estopa, R.A.; Paludeto, J.G.Z.; Müller, B.S.F.; de Oliveira, R.A.; Azevedo, C.F.; de Resende, M.D.V.; Tambarussi, E.V.; Grattapaglia, D. Genomic Prediction of Growth and Wood Quality Traits in *Eucalyptus benthamii* Using Different Genomic Models and Variable Snp Genotyping Density. *New For.* **2023**, *54*, 343–362. [[CrossRef](#)]
89. Duarte, D.; Jurcic, E.J.; Dutour, J.; Villalba, P.V.; Centurión, C.; Grattapaglia, D.; Cappa, E.P. Genomic Selection in Forest Trees Comes to Life: Unraveling Its Potential in an Advanced Four-Generation *Eucalyptus grandis* Population. *Front. Plant Sci.* **2024**, *15*, 1462285. [[CrossRef](#)]
90. Giorello, F.M.; Farias, J.; Basile, P.; Balmelli, G.; Da Silva, C.C. Evaluating the Potential of Xp-Gwas in *Eucalyptus*: Leaf Heteroblasty as a Case Study. *Plant Gene* **2023**, *36*, 100430. [[CrossRef](#)]
91. Rocha, L.F.; Benatti, T.R.; de Siqueira, L.; de Souza, I.C.G.; Bianchin, I.; de Souza, A.J.; Fernandes, A.C.M.; Oda, S.; Stape, J.L.; Yassue, R.M.; et al. Quantitative Trait Loci Related to Growth and Wood Quality Traits in *Eucalyptus grandis* W. Hill Identified through Single- and Multi-Trait Genome-Wide Association Studies. *Tree Genet. Genomes* **2022**, *18*, 38. [[CrossRef](#)]

Disclaimer/Publisher’s Note: The statements, opinions and data contained in all publications are solely those of the individual author(s) and contributor(s) and not of MDPI and/or the editor(s). MDPI and/or the editor(s) disclaim responsibility for any injury to people or property resulting from any ideas, methods, instructions or products referred to in the content.